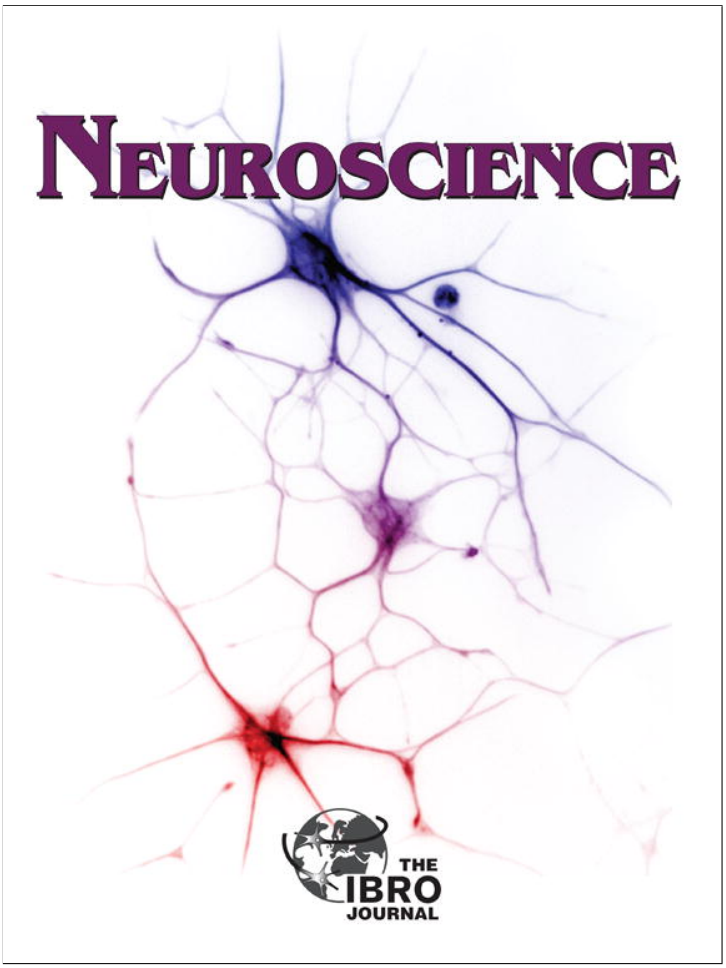

Neuroscience 241 (2013) 170–187

REARRANGEMENT OF THE DENDRITIC MORPHOLOGY IN LIMBIC REGIONS AND ALTERED EXPLORATORY BEHAVIOR IN A RAT MODEL OF AUTISM SPECTRUM DISORDER

M. E. BRINGAS,[a] F. N. CARVAJAL-FLORES,[a] T. A. LÓPEZ-RAMÍREZ,[c] M. ATZORI[b,d] AND G. FLORES[a]*

[a] *Laboratorio de Neuropsiquiatría, Instituto de Fisiología, Universidad Autónoma de Puebla, Puebla, Mexico*

[b] *Laboratory of Synaptic and Cellular Physiology, School of Behavioral and Brain Sciences, University of Texas at Dallas, USA*

[c] *Depto. de Ciencias Químico Biológicas, Escuela de Ciencias, Universidad de las Américas-Puebla, Mexico*

[d] *Lab. de Fisiología Celular y Sináptica, Inst. de Física, Univ. Autónoma de San Luis Potosí, San Luis Potosí, Mexico*

Abstract—Valproic acid (VPA) is a blocker of histone deacetylase widely used to treat epilepsy, bipolar disorders, and migraine; its administration during pregnancy increases the risk of autism spectrum disorder (ASD) in the child. Thus, prenatal VPA exposure has emerged as a rodent model of ASD. In the present study, we aimed to investigate the effect of prenatal administration of VPA (500 mg/kg) at E12.5 on the exploratory behavior and locomotor activity in a novel environment, as well as on neuronal morphological rearrangement in the prefrontal cortex (PFC), in the hippocampus, in the nucleus accumbens (NAcc), and in the basolateral amygdala (BLA) at three different ages: immediately after weaning (postnatal day 21 [PD21]), prepubertal (PD35) and postpubertal (PD70) ages. Hyper-locomotion was observed in a novel environment in VPA animals at PD21 and PD70. Interestingly, exploratory behavior assessed by the hole board test at PD70 showed a reduced frequency but an increase in the duration of head-dippings in VPA-animals compared to vehicle-treated animals. In addition, the latency to the first *head-dip* was longer in prenatal VPA-treated animals at PD70. Quantitative morphological analysis of dendritic spine density revealed a reduced number of spines at PD70 in the PFC, dorsal hippocampus and BLA, with an increase in the dendritic spine density in NAcc and ventral hippocampus, in prenatal VPA-treated rats. In addition, at PD70 increases in neuronal arborization were observed in the NAcc, layer 3 of the PFC, and BLA, with retracted neuronal arborization in the ventral and dorsal hippocampus. Our results extend the list of altered behaviors (exploratory behavior) detected in this model of ASD, and indicate that the VPA behavioral phenotype is accompanied by previously undescribed morphological rearrangement in limbic regions.

Key words: valproic acid, prefrontal cortex, hippocampus, nucleus accumbens, amygdala, autism.

INTRODUCTION

Autism spectrum disorders (ASDs) are neurodevelopmental disorders characterized by pervasive abnormalities in social interaction and communication, repetitive behavioral patterns and restricted interests (APA, 1994, DSMIV). The first report of dysfunctional connectivity between cortical and subcortical regions in ASD came from Horwitz et al. (1988). Interestingly, in recent years, the study of connectivity in ASD has increased its attention (for review see Wass, 2011). In addition, a considerable number of neuroimaging studies have suggested that long-distance connectivity is disrupted in ASD (for review see Wass, 2011). Functional magnetic resonance imaging (MRI) and electroencephalography (EEG) studies in mature subjects with ASD suggested overwhelming evidence of functional under-connectivity (Rippon et al., 2007; Casanova and Trippe, 2009). In younger subjects with ASD, there are scant reports with mixed evidence (Casanova and Trippe, 2009). Interestingly, the under-connectivity theory suggests that autism is a cognitive and neurobiological disorder marked and possibly caused by under-functioning long-distance integrative circuitry, eventually resulting in a deficit of integration of information at the neural and cognitive levels (for review see Wass, 2011). Specifically, prefrontal cortex (PFC) damage may result in impaired social behavior, which is a distinctive feature of ASD patients (for review see Shalom, 2009; Thompson et al., 2010). The prenatal valproic acid (VPA) exposure has been proposed as a neurodevelopmental model of ASD-like behavioral abnormalities in the rat (Rodier et al., 1997; Ingram et al., 2000; Markram and Markram, 2010). These behaviors include hyper-responsiveness to novel environment (Schneider and Przewłocki, 2005), deficits in sensory gating and social interaction (Schneider et al., 2006), and stereotyped or repetitive behaviors (Schneider and Przewłocki, 2005). Additionally, prenatal VPA exposure induces neuronal rearrangements (Snow

*Corresponding author. Address: Laboratorio de Neuropsiquiatría, Instituto de Fisiología, Universidad Autónoma de Puebla, 14 Sur 6301, Puebla CP 72570, Mexico. Tel: +52-222-295500x7322; fax: +52-222-295500x7301.
E-mail addresses: gonzaloflores56@gmail.com, gonzalo.flores@correo.buap.mx (G. Flores).

Abbreviations: ASD, autism spectrum disorder; BLA, basolateral amygdala; DA, dopamine; DA transporter, DAT; MD, mediodorsal; NAcc, nucleus accumbens; NLGNs, neuroligins; NRXN, neurexin; OBX, olfactory bulbectomy; PD, postnatal day; PFC, prefrontal cortex; TDL, total dendritic length; VPA, valproic acid.

0306-4522/13 $36.00
http://dx.doi.org/10.1016/j.neuroscience.2013.03.030

et al., 2008; Mychasiuk et al., 2012), altered serotoninergic (5HT) transmission (Miyazaki et al., 2005; Dufour-Rainfray et al., 2010), impairment of GABAergic transmission in the temporal cortex (Banerjee et al., 2012) and deregulated expression of proteins including neuroligin 3 and associated with neurotransmitter release (Kolozsi et al., 2009), as observed in autism patients.

PFC sends excitatory projections to several cortico-limbic regions including the nucleus accumbens (NAcc) (Jay and Witter, 1991). Recent reports suggest that adult rats with prenatal VPA exposure show a neural loss and atrophy in the PFC (Mychasiuk et al., 2012; Hara et al., 2012). However, comparatively few studies have investigated other limbic structures such as the basolateral amygdala (BLA) and the hippocampus, which are interconnected through the PFC, play a critical role in memory and emotional processing (Chen et al., 2011), and are often disturbed in ASD subjects (for review see Shalom, 2009; Thompson et al., 2010; Lauvin et al., 2012). A critical involvement of limbic areas in ASD pathophysiology is corroborated by abnormalities in the dopaminergic and glutamatergic system, paralleled by similar deficits in the VPA model (McCracken et al., 2002; Denys et al., 2004) as well as in the prenatal VPA exposure (Rinaldi et al., 2007; Schneider et al., 2007).

In order to test a cognitive feature associated with a strong limbic component we evaluated the effect of prenatal VPA administration on locomotor activity in novel environment and exploratory behavior in rats at three different ages immediately after weaning (postnatal day 21 [PD21]), prepubertal (PD35) and postpubertal (PD70) ages. Additionally, we evaluated neuronal arborization in key brain regions involved in autism-related behavior in this model.

EXPERIMENTAL PROCEDURES

Animals

Pregnant Sprague–Dawley rats were obtained at gestational day 10 from our facilities (University of Puebla, Mexico). Rats were individually housed in a temperature and humidity controlled environment on a 12-h–12-h light–dark cycle with free access to food and water. All procedures described in the present study were in agreement with the ''Guide for Care and Use of Laboratory Animals'' of the Mexican Council for Animal Care (Norma Oficial Mexicana NOM-062-ZOO-1999) and the National Institutes of Health Guide for the Care and Use of Laboratory Animals. All efforts were made to minimize animal suffering and the number of animals used in this study.

Prenatal VPA exposure

VPA (Sigma–Aldrich, St. Louis, MO, USA) was purchased as the sodium salt and dissolved in 0.9% saline at a concentration of 250 mg/ml. Females received a single intraperitoneal injection of 500 mg/kg sodium valproate (VPA) or physiological saline (vehicle) on E12.5 as previously described (Schneider and Przewlocki, 2005; Rinaldi et al., 2007; Hara et al., 2012; Kataoka et al., 2013). Unchanged litter size, pup body weight, and general health of the mothers and pups (data not shown) were indications of normal rearing conditions for treated rats. Females raised their own litters. Male offspring were weaned on postnatal day 21 (PD21). No more than three siblings were housed together in cages. Vehicle rats and VPA-treated rats were housed in separate cages. Animals had free access to food and water.

Spontaneous locomotor activity in a novel environment

Tests were made as described in detail previously (Flores et al., 1996b; Flores-Tochihuitl et al., 2008; Monroy et al., 2010). The locomotor activity was monitored for 120 min in 16 individual cages (20 × 40 × 30 cm), each of which was equipped with an eight-photo-beam detector connected to a computer counter (Tecnologia Digital, Mexico). The locomotor activity was evaluated in independent groups of animals at PD21, PD35 and PD70 in vehicle and VPA animals.

Neuronal rearrangement quantification

To evaluate possible neuronal rearrangement in autism-related regions including PFC, NAcc, hippocampus and BLA, the Golgi–Cox method was used on PD21, PD35 and PD70 to quantify the dendritic arborization and neuronal spine density. Immediately after measuring the locomotor activity, rats from the two treatments were anesthetized with sodium pentobarbital (60 mg/kg body weight, i.p.) and perfused intracardially with saline solution. Brains were removed and stained by modified Golgi–Cox method as described previously (Gibb and Kolb, 1998; Flores et al., 2005b; Juárez et al., 2008; Alcantara-Gonzalez et al., 2010; Bringas et al., 2012). Coronal sections of 200-μm thickness from the PFC, hippocampus, BLA and NAcc were obtained using a vibratome (Campden Instruments, MA752, Leicester, UK). These sections were collected on clean gelatin-coated microscope slides and treated with ammonium hydroxide for 30 min, followed by 30 min in Kodak Film Fixer and subsequently washed with distilled water, dehydrated and cleared in successive baths of 50% (1 min), 70% (1 min), 95% (1 min), and 100% (2 × 5 min) ethanol followed by 15 min in a xylene solution. Subsequently, the slides were covered with balsam resinous medium.

Pyramidal cells from PFC layer 3 and 5 (area Cingulate1 and prelimbic cortex, plates 7–9), pyramidal neurons from ventral (plates 37–42) and dorsal hippocampus (plates 27–33), NAcc medium spiny neurons (plates 10–13) and pyramidal neurons from BLA (plates 27–31) were selected for study according to the Paxinos and Watson Atlas (1986). For each animal, neurons from both the left and right PFC, hippocampus, BLA and NAcc were drawn using camera lucida at a magnification of 400× (DMLS, Leica Microscope) by a trained observer who was blinded to the experimental conditions (Kolb et al., 1997, 1998). Pyramidal neurons were identified by their characteristic triangular soma-shape, apical dendrites extending toward the pial surface and numerous dendritic spines. Medium spiny neurons of the NAcc were recognized by their soma size and dendritic extensions. Sequential two-dimensional reconstruction of the entire dendritic tree was generated for each neuron and the dendritic tracings were quantified by Sholl analysis (Sholl, 1953; Flores et al., 2005a; Juárez et al., 2008; Morales-Medina et al., 2009; Martínez-Téllez et al., 2009). A transparent grid with equidistant (10 μm) concentric rings was centered over the dendritic tree tracings and the number of ring intersections was used to estimate the total dendritic length (TDL) and dendritic arborization (Fig. 1). The estimate of the total number of dendritic branches (branching indicated by Y bifurcation) was counted at each order away from the cell body or dendritic shaft. To calculate the spine density, the length of dendrite (⩾10-μm long) was traced at 1000×, and the number of spines along this dendritic segment was counted (spines/10 μm).

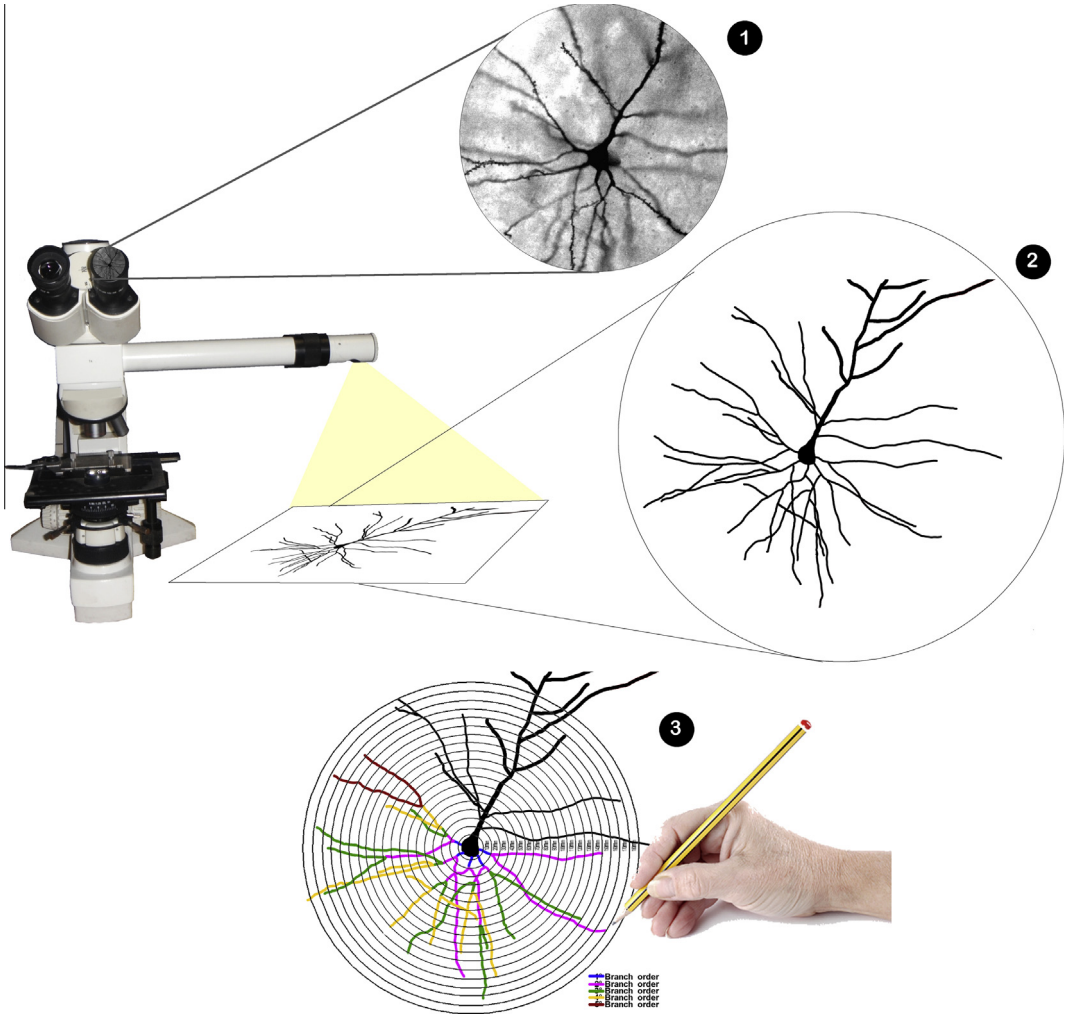

Fig. 1. Sholl analysis. For each neuron, the three-dimensional dendritic tree, including all branches (1), was reconstructed in a two-dimensional plane by using camera lucida (2) and the dendritic tracing was quantified by Sholl analysis (Sholl, 1953). A transparent grid with equidistant (10 μm) concentric rings was centered over the dendritic tree tracings and the number of ring intersections was used to estimate the total dendritic length and dendritic branch order (3).

Hole-board apparatus

The hole-board experiments were made by using an automatic hole-board apparatus (Tecnología Digital, Mexico) consisting of a black acrylic box (50 × 50 × 30 cm) with one equidistant hole (3.8-cm diameter) in one of the walls. An infrared beam sensor was installed on the wall to detect the number and duration of the head dipping behavior.

Effect of the prenatal VPA-exposure on the exploratory behavior of rat in the hole-board test

Another cohort of animals was used to study the hole-board test (n = 7–8 animals per group). Each animal was handled for 5 min on the day prior to initial (preoperative) test. The head-dipping activity was assessed in vehicle and prenatal VPA-exposed rats by the following condition: On the first to the fifth day each rat was placed facing a random direction in the center of the apparatus and allowed to freely explore the apparatus for 10 min. The total number and duration of head-dipping were automatically recorded.

Statistical analysis

The mean values for each brain region were treated as a single measurement for the data analysis (n = 7–9, neuronal rearrangement quantification). Locomotor activity induced by novel environment, data of the *hole-board test*, dendritic length and spine density data were analyzed by a two-way ANOVA followed by the Newman–Keuls test for post hoc comparisons using age and prenatal VAP exposure as independent factors. The data for the length per branch order were also analyzed by a two-way ANOVA, followed by the Newman–Keuls test for post hoc comparisons, with prenatal VPA exposure and branch order as independent factors. $P < 0.05$ was considered significant in all tests.

RESULTS

Behavioral data

Locomotor activity. Both vehicle- and prenatal VPA-exposed animals initially showed increased locomotor activity reflecting active exploratory behavior in a novel

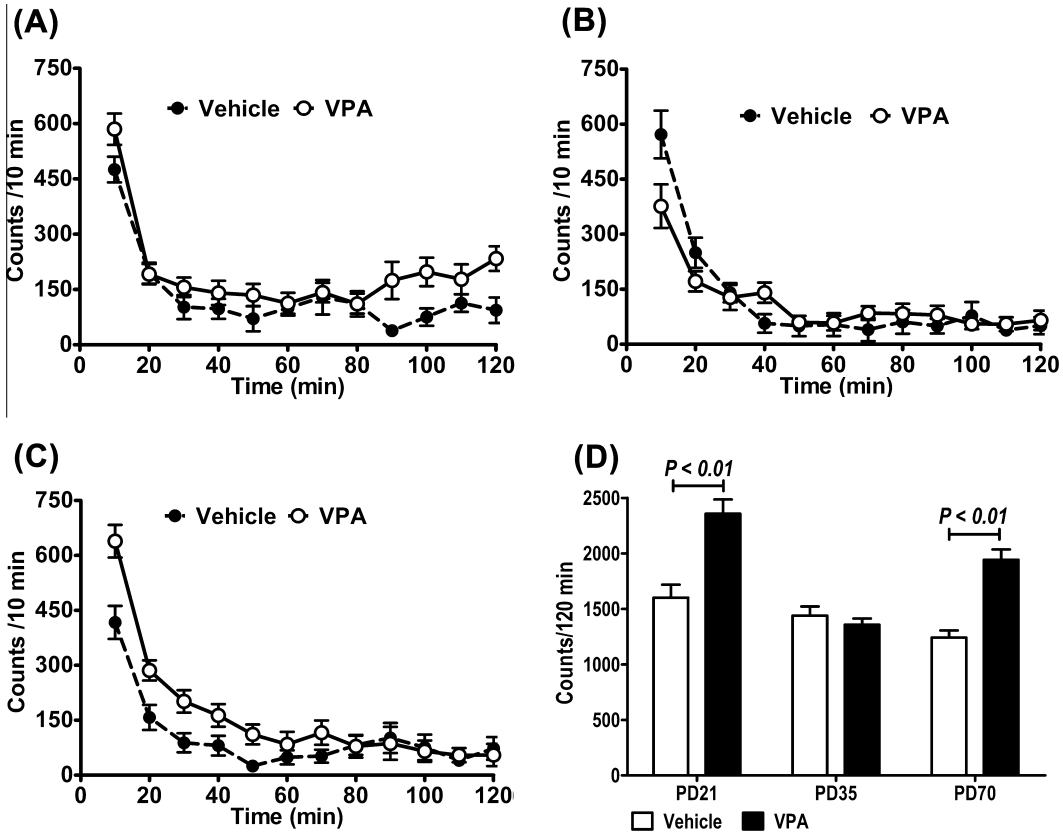

Fig. 2. Locomotor activity (mean number of beam interruption per 10 min ± SEM, $n = 9$ per group) in a novel environment of vehicle-treated and VPA-treated animals tested at PD21, PD35 and PD70. Temporal profile of the locomotor activity at PD21 (A), PD35 (B) and PD70 (C). (D) Analysis of total activity scores reveals that VPA-treated animals are more active compared to their corresponding vehicle-treated rats at PD21 and PD70.

environment. The locomotor activity gradually declined to a stable level in 30 min in the vehicle and prenatal VPA animals at P21 and PD35, however, in prenatal VPA-exposure animals at PD70 (Fig. 2A), locomotion reached a stable level in 60 min compared to vehicle animals (Fig. 2A). An analysis of the data for the entire 120-min period (two-way ANOVA, VPA: $F_{1,48} = 35$, $P < 0.01$; age: $F_{2,48} = 19$, $P < 0.001$; VPA vs. age: $F_{2,48} = 12$, $P < 0.001$) showed a significant increase in locomotor activity in prenatal VPA-exposed animals at PD21 and PD70 compared to the vehicle rats (Fig. 2B).

Effect of prenatal VPA exposure on exploratory behavior

The effect of prenatal VPA exposure on exploratory behavior is shown in Fig. 2A–C. The duration (3A) of head-dipping behaviors in prenatal VPA-exposed rats (two-way ANOVA, VPA: $F_{1,37} = 6.9$, $P = 0.01$; age: $F_{2,37} = 26$, $P < 0.001$; VPA vs. age: $F_{2,37} = 9.1$, $P < 0.001$) was significantly longer than in vehicle animals ($P < 0.01$) only at PD70. Whereas the number (3B) of head-dippings (two-way ANOVA, VPA: $F_{1,37} = 14$, $P < 0.01$; age: $F_{2,37} = 11$, $P < 0.001$; VPA vs. age: $F_{2,37} = 3.6$, $P < 0.05$) was significantly lower in prenatal VPA-exposed rats compared to vehicle animals only at PD70 ($P < 0.01$). In addition, in prenatal VPA-exposed animals at PD70, the latency to the first head dip was significantly longer compared to control animals (two-way ANOVA, VPA: $F_{1,37} = 9.9$, $P < 0.01$; age: $F_{2,37} = 4.3$, $P = 0.01$; VPA vs. age: $F_{2,37} = 5.5$, $P < 0.01$) ($P < 0.01$, Fig. 3C).

Prenatal VPA-exposure causes neuronal rearrangement in PFC, NAcc, hippocampus and BLA

The morphological analysis presented here is based on a total of 3180 neurons from 48 animals. Estimates of dendritic length and spine density were obtained from 960 PFC and 480 dorsal and 480 ventral hippocampal CA1 pyramidal neurons, 420 BLA neurons and from 840 NAcc medium spiny neurons. Thus, 320 PFC, 320 hippocampal CA1 pyramidal, 280 NAcc medium spiny neurons and 140 BLA pyramidal neuronal were analyzed for each of the three ages (PD21, PD35 and PD70, $n = 7$–8 animals per age); between 70 and 80 neurons were analyzed for each of the two conditions (Vehicle and VPA-exposure) by postnatal age ($n = 3$). Table 1 details the number of neurons and animals analyzed for each group and postnatal age.

As observed in our previous studies, the Golgi–Cox impregnation procedure clearly filled the dendritic shafts and spines of layer III and V pyramidal neurons of the PFC, medium spiny neurons of the NAcc and pyramidal neurons of the dorsal and ventral hippocampus and BLA (Silva-Gomez et al., 2003; Flores et al., 2005a,b;

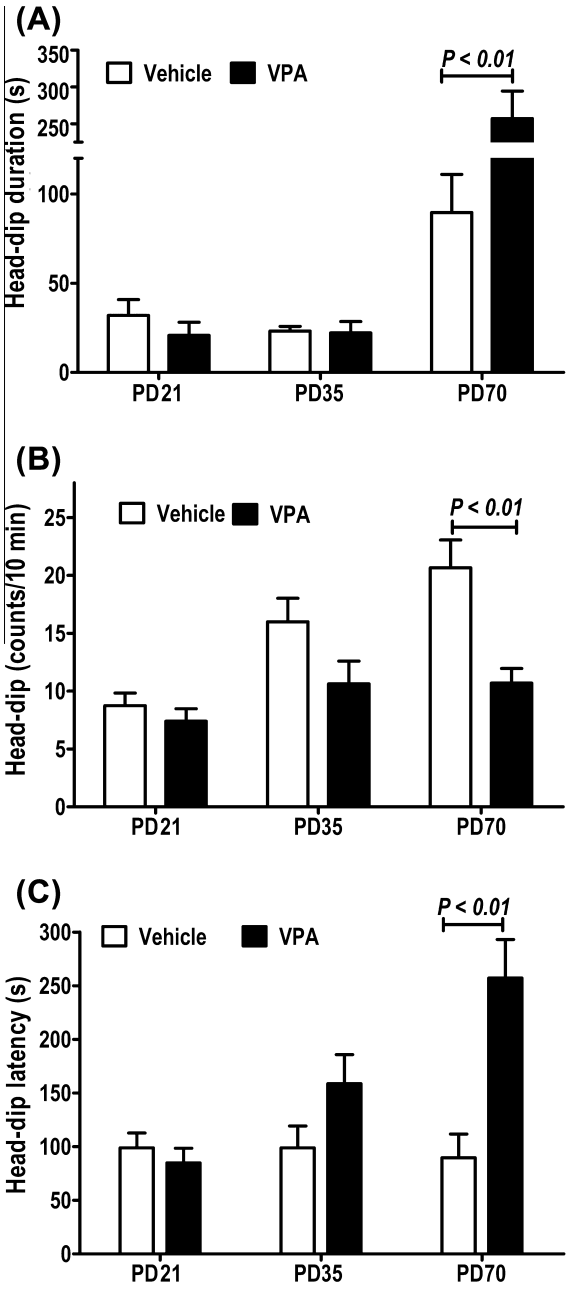

Fig. 3. The effect of prenatal valproic acid (VPA) exposure on the exploratory behavior in rats tested at PD21, PD35 and PD70 on the hole-board. Each column represents the means with S.E. of 8 (VPA) to 7 (vehicle) rats. The duration (A) and number (B) of head-dipping behaviors. In addition, the latency to the first head dip (C).

Morales-Medina et al., 2009; Martínez-Téllez et al., 2009; Torres-García et al., 2012). Examples of impregnated PFC, hippocampus, BLA and NAcc neurons from vehicle animals at PD70 are shown in Figs. 4 and 5.

In agreement with previous report (Hara et al., 2012; Mychasiuk et al., 2012), in PFC layer 3, prenatal VPA-exposure induces spine loss for all ages studied with dendritic retraction at PD21 ($P < 0.01$), which at PD70 ($P < 0.05$) was converted to dendritic hypertrophy (Fig 6A–C, two-way ANOVA, VPA, $F_{1,42} = 123$, $P < 0.001$, age, $F_{2,42} = 6.1$, $P < 0.01$, dendritic length and age vs. VPA, $F_{2,42} = 9.6$, $P < 0.001$, age, $F_{2,42} = 50$, $P < 0.001$, spines). Another measure obtained from the Sholl analysis was the length per branch order. Branch-order analysis (two-way ANOVA, VPA: $F_{5,252} = 8.4$, $P < 0.001$; Branch order: $F_{5,252} = 593$, $P < 0.001$; VPA vs. age: $F_{25,252} = 3.9$, $P < 0.001$) indicated that dendritic length of layer 3 PFC were decreased in VPA-treated animals at the level of the third ($P < 0.01$) order at PD21, with an increase in VPA-treated rats at the level of the first and third orders at PD70 ($P < 0.05$, Fig 6F), whereas in the PFC layer 5, prenatal VPA-exposure only induces a decreases in the dendritic spine density at all studies age (Fig 7B, VPA, $F_{1,42} = 126$, $P < 0.001$) without changes in dendritic length (Fig. 7C).

Interestingly, the TDL of pyramidal neurons of CA1 in the dorsal and ventral hippocampus (VPA, $F_{1,42} = 24$, $P < 0.001$, age, $F_{2,42} = 8.9$, $P < 0.001$, age vs. VPA, $F_{2,42} = 2.6$, $P = 0.08$, dorsal hippocampus; age, $F_{2,42} = 3.3$, $P = 0.04$, VPA, $F_{1,42} = 12.8$, $P < 0.001$, ventral hippocampus) was decreased in prenatal VPA-exposed animals at PD70 (Figs. 8C and 9C). In addition, an increase in dendritic spine density was observed in VPA-treated rats at PD21 ($P < 0.05$) in the dorsal hippocampus (Fig. 8B, age vs. VPA, $F_{2,42} = 9.3$, $P < 0.001$) and at all ages ($P < 0.05$) in the ventral hippocampus (Fig. 9B, age, $F_{2,42} = 14$, $P < 0.001$, VPA, $F_{1,42} = 22$, $P < 0.001$), with a decrease in the dendritic spine density at PD70 ($P < 0.05$) in the dorsal hippocampus (Fig. 8B). Branch-order analysis indicated that dendritic length of both dorsal and ventral hippocampus were decreased in the VPA-treated animals (two-way ANOVA, VPA: $F_{5,328} = 25.9$, $P < 0.01$; branch order: $F_{7,328} = 763$, $P < 0.001$; VPA vs. age: $F_{35,328} = 3.8$, $P < 0.001$, dorsal hippocampus; VPA: $F_{5,336} = 16$, $P < 0.001$; branch order: $F_{7,336} = 497$, $P < 0.001$; VPA vs. age: $F_{35,336} = 3..4$, $P < 0.001$, ventral hippocampus), at the level of the third to sixth ($P < 0.01$) orders in the dorsal hippocampus and third to seventh ($P < 0.01$) orders in the ventral hippocampus only at PD70.

Both parts of the NAcc, core and shell, responded in a similar manner to the prenatal VPA exposure: hypertrophy ($P < 0.01$) of the dendritic length at PD35 ($P < 0.05$, core; $P < 0.01$ shell) and PD70 ($P < 0.01$) compared to vehicle-treated (VPA, $F_{1,36} = 4.1$, $P = 0.03$, age, $F_{2,36} = 26$, $P < 0.001$, age vs. VPA, $F_{2,36} = 8.6$, $P < 0.001$, core; VPA, $F_{1,36} = 19$, $P < 0.001$, age, $F_{2,36} = 15$, $P < 0.001$, age vs. VPA, $F_{2,36} = 34$, $P < 0.001$, shell) (Figs. 10D and 11D). Interestingly, at PD21, we observed a hypotrophy of the dendritic length ($P < 0.01$) in the NAcc shell (Fig. 10D). We further evaluated spine density at two different levels (the second branch order and the distal branch order) in these NAcc neurons. Prenatal VPA treatment increased spine density at both levels evaluated (Fig. 10B, C, respectively) (NAcc core: VPA, $F_{1,36} = 147$, $P < 0.001$, age, $F_{2,36} = 66$, $P < 0.001$, second order and VPA, $F_{1,36} = 67$, $P < 0.001$; age, $F_{2,36} = 89$, $P < 0.001$, VPA vs. age, $F_{2,36} = 22$, $P < 0.001$, distal. NAcc shell (Fig. 11B, C): VPA, $F_{1,36} = 64$, $P < 0.001$, age,

Table 1. Number of neurons and of animals analyzed per VPA group and postnatal age

	21PN		35PN		70PN		No. of neurons
	Vehicle (n = 8)	VPA (n = 8)	Vehicle (n = 8)	VPA (n = 8)	Vehicle (n = 8)	VPA (n = 8)	
PFC Layer III	80	80	80	80	80	80	480
PFC Layer V	80	80	80	80	80	80	480
DH	80	80	80	80	80	80	480
VH	80	80	80	80	80	80	480
Nacc-Shell	70	70	70	70	70	70	420
Nacc-Core	70	70	70	70	70	70	420
BLA	70	70	70	70	70	70	420
Total no. of neurons/No. of animals							3180/48

Ten neurons from each brain region (5/hemisphere) of each animal were analyzed and the mean values from each brain region of each animal were treated as single measurements for the data analysis.

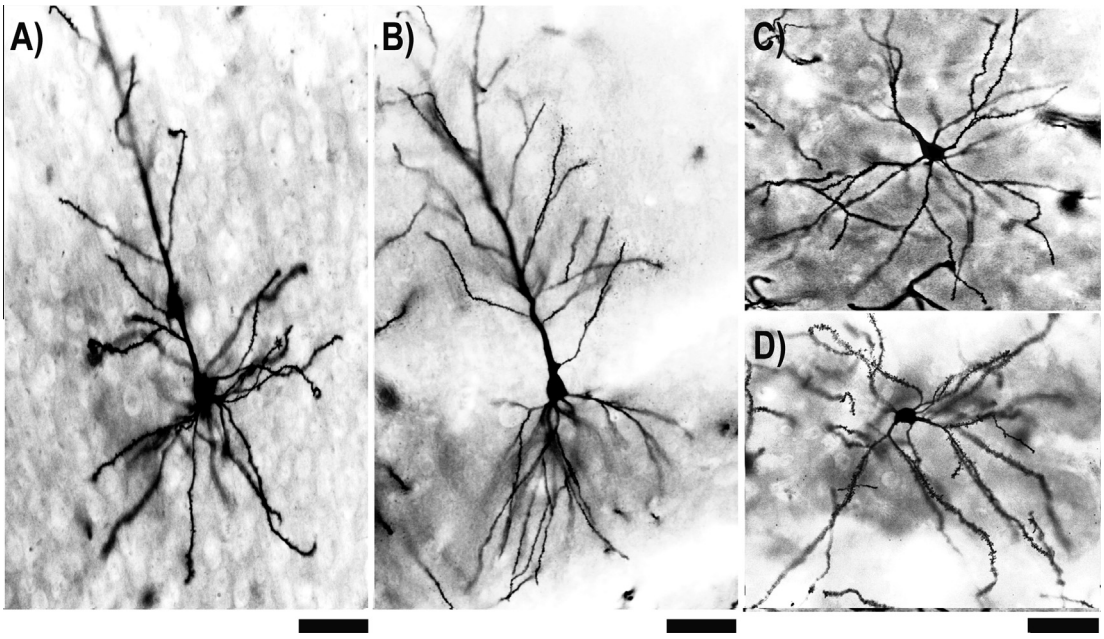

Fig. 4. Photomicrographs showing a representative Golgi–Cox-impregnated pyramidal neurons of the PFC (A), dorsal hippocampus (B), and BLA (C), and medium spiny neuron of the NAcc (D) from vehicle-treated animal. Bar = 100 μm.

$F_{2,36}$ = 80, P < 0.001, VPA vs. age, $F_{2,36}$ = 17, P < 0.001, second order and VPA, $F_{1,36}$ = 69, P < 0.001; age, $F_{2,36}$ = 36, P < 0.001, VPA vs. age, $F_{2,36}$ = 29, P < 0.001, distal. Prenatal VPA treatment increased spine density (P < 0.01) selectively in second order segments at PD21 and PD70 in the NAcc shell and at all the ages in the NAcc core (Figs. 10B and 11B). Similarly, an increase in the number of spines in distal sections of the prenatal VPA animals was observed at PD21 and PD70 in both parts of the NAcc (Figs. 10C and 11C, P < 0.01). Branch order analysis showed that selective increases at the level of the fourth (P < 0.01) order in the NAcc core at PD35 and PD70 (Fig. 10F, G), at the level of the third and fourth (P < 0.01) orders at PD35 (Fig. 11F), and at the level of the fifth (P < 0.01) order at PD70 (Fig. 11G) in the NAcc shell in the prenatal VAP-exposed rat compared to vehicle rats (two-way ANOVA, VPA: $F_{5,252}$ = 9.1, P < 0.01; branch order: $F_{6,252}$ = 694, P < 0.001; VPA vs. age: $F_{30,252}$ = 3.4, P < 0.001, core; VPA: $F_{5,245}$ = 14, P < 0.001; branch order: $F_{6,245}$ = 691, P < 0.001; VPA vs. age: $F_{30,245}$ = 3.7, P < 0.001, shell). Interestingly, at PD21, prenatal VPA treatment reduced the dendritic length at the level of the third (P < 0.01) order in the NAcc shell (Fig. 11E).

Prenatal VPA exposure also changed in different ways the TDL and spine density in BLA pyramidal neurons (Fig. 12) (VPA, $F_{1,36}$ = 4.1, P = 0.05, age, $F_{2,36}$ = 74, P < 0.001, VPA vs. age, $F_{2,36}$ = 8.6, P < 0.001, TDL, VPA, $F_{1,36}$ = 33, P < 0.001, age, $F_{2,36}$ = 180, P < 0.001, VPA vs. age, $F_{2,36}$ = 86, P < 0.001, second order and age, $F_{2,36}$ = 79, P < 0.001, VPA vs. age, $F_{2,36}$ = 81, P < 0.001, distal). At PD21, prenatal VPA treatment enhanced number of spines of both

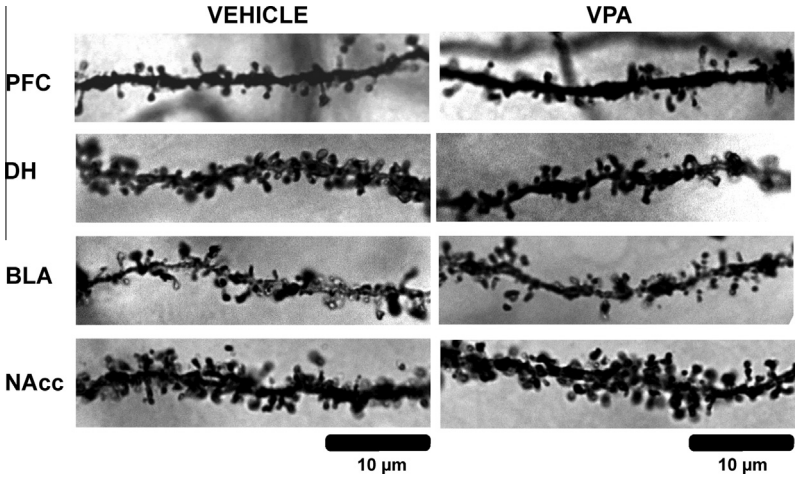

Fig. 5. Photomicrographs showing a representation of Golgi–Cox-impregnated dendritic spines of the neurons from VPA-treated and vehicle-treated animal at PD70.

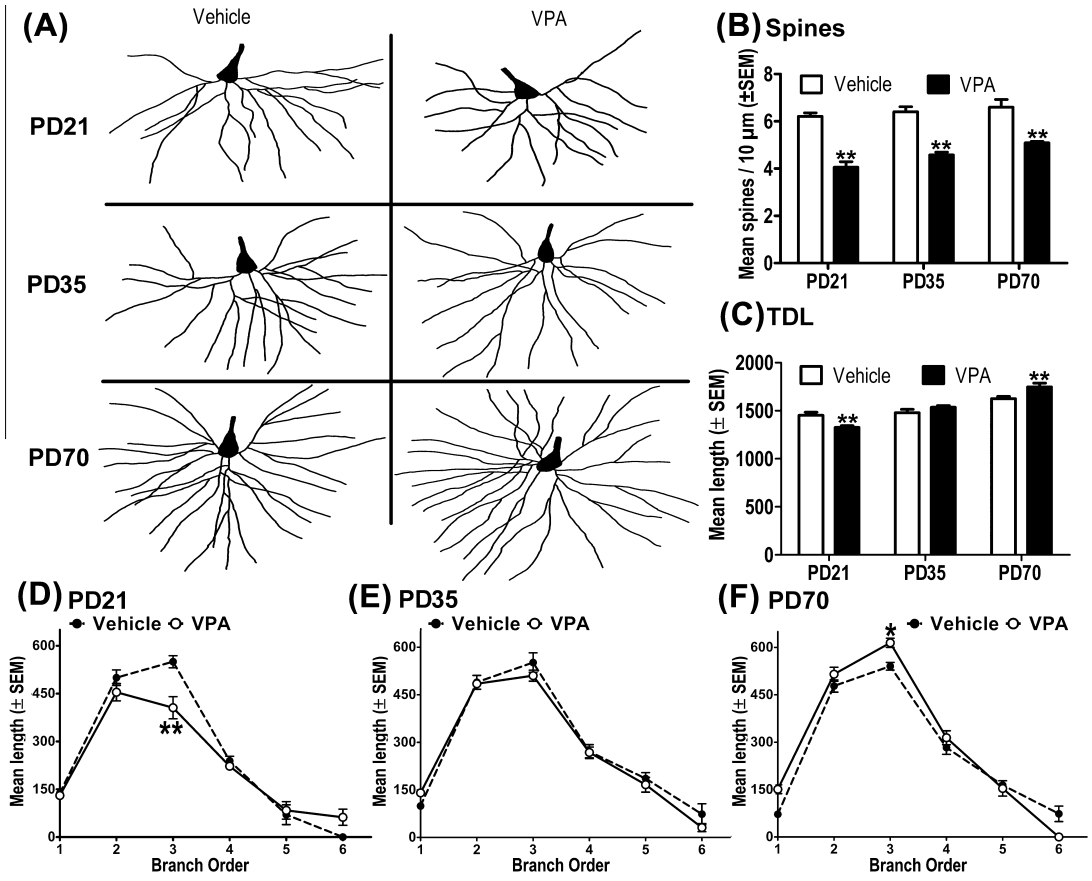

Fig. 6. Analysis of the prenatal valproic acid (VPA) effect on the pyramidal neurons from layer III of the prefrontal cortex (PFC) immediately after weaning (PD21), in prepubertal (PD35) and in postpubertal (PD70) animals (n = 8–9 animals per group). (A) Representative schematic drawings of the dendritic basilar arbor of the PFC neurons. (B) Dendritic spiny neuron density. The density of the dendritic spines decreased in VPA-treated animals compared to their corresponding vehicle rats at all ages. (C) Total dendritic length (TDL) analysis also revealed that VPA-treated rats showed an atrophy of the TDL at PD21 with an increase in the arbor at PD70 compared to their corresponding vehicle animals. Interestingly, at prepubertal age significantly ameliorated the dendritic length hypotrophy observed at PD21 in the pyramidal neurons of the PFC of the VPA-treated rats. (D–F) Length of branch-order analysis revealed that dendritic length of the layer III of the PFC was shorter in the VPA-treated animals at the level of the third order compared to vehicle-treated rats at PD21. Whereas at PD35, no differences were observed and at PD70, the dendritic length was enhanced at the level of the third order compared to vehicle-treated rats. $^{*}P < 0.05$, $^{**}P < 0.01$.

localization (Fig. 12B, C, $P < 0.01$), but at PD35 the increases in the number of spines was present only in the second order localization ($P < 0.01$) in BLA neurons compared to vehicle animals (Fig. 12B), while at PD70

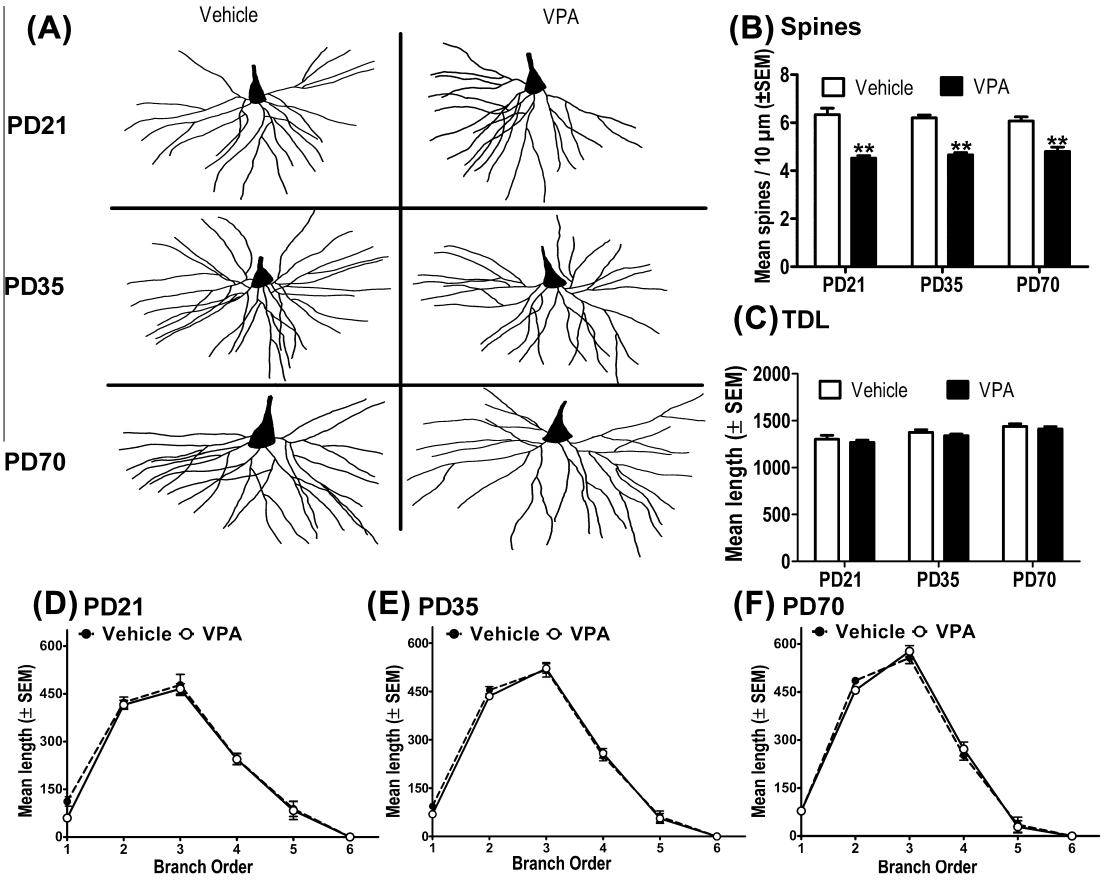

Fig. 7. The prenatal valproic acid (VPA) effect on the pyramidal neurons from layer V of the prefrontal cortex (PFC) immediately after weaning (PD21), in prepubertal (PD35) and in postpubertal (PD70) animals (n = 8 animals per group). (A) Representative schematic drawings of the dendritic basilar arbor of the PFC neurons. (B) Dendritic spine number analysis revealed that prenatal VPA exposure animals showed a reduced spinogenesis compared to their corresponding vehicle rats at all ages. (C) Total dendritic length analysis revealed that there are no differences among groups. (D–F) Length of branch-order analysis revealed that that there are no differences among groups. $^{*}P < 0.05$, $^{**}P < 0.01$.

an increased TDL ($P < 0.01$) with a reduced number of spines ($P < 0.01$) was observed in the prenatal VPA exposure rats (Fig. 12B, C and D). In addition, in the branch order analysis in the BLA (two-way ANOVA, VPA: $F_{5,238} = 19.5$, $P < 0.01$; branch order: $F_{6,238} = 698$, $P < 0.001$; VPA vs. age: $F_{30,238} = 3$, $P < 0.01$), we observed a decrease at the level of the third to fourth orders (third $P < 0.01$; fourth $P < 0.05$) in the prenatal VPA rat at PD21 compared to vehicle rats (Fig. 12E). Interestingly, this dendritic atrophy was throwback with the age, because at PD35 and PD70, the BLA neurons of the VPA-treated animals showed an increase at the level of the fifth and third order, respectively (fifth $P < 0.05$; PD35 and third $P < 0.01$, PD70) (Fig. 12F, G).

DISCUSSION

The present study demonstrates that the antiepileptic agent VPA administered prenatally produces behavioral alterations in the novel environment-induced locomotion and exploratory behavior tested by Hole-board procedure further supporting its value as a neurodevelopmental model of ASD. The behavioral alterations in the locomotion and exploratory behavior test observed in this study are consistent with previous studies using this model (Schneider and Przewłocki, 2005; Wagner et al., 2006; Nakasato et al., 2008; Dufour-Rainfray et al., 2010; Sui and Chen, 2012) and are reminiscent of the behavioral disturbances in patients with autism (for review see Wass, 2011). Consistent with the behavioral data, morphological examination of the limbic subregions in this animal model found that prenatal VPA exposure also alter the dendritic morphology. However the dendritic changes are complex. A reduced number of spines was observed in the pyramidal neurons of the PFC at all studied ages, in the dorsal hippocampus and the BLA at PD70. In contrast, an increase in the dendritic spine density was observed in pyramidal neurons of the ventral hippocampus at all studied ages and in the BLA at PD21 and PD35, and in medium spiny neurons of the NAcc at all ages in the core part and PD21 and PD70 to the shell part. Interestingly, pyramidal neurons of the dorsal and ventral hippocampus at PD35 and PD70, and BLA and PFC at early age, PD21, showed a dendritic short-distance (arborization) hypotrophy, however medium spiny neurons of the NAcc at PD35 and PD70 and pyramidal neurons of the PFC and BLA at adult age, PD70, exhibited a dendritic short-distance hypertrophy.

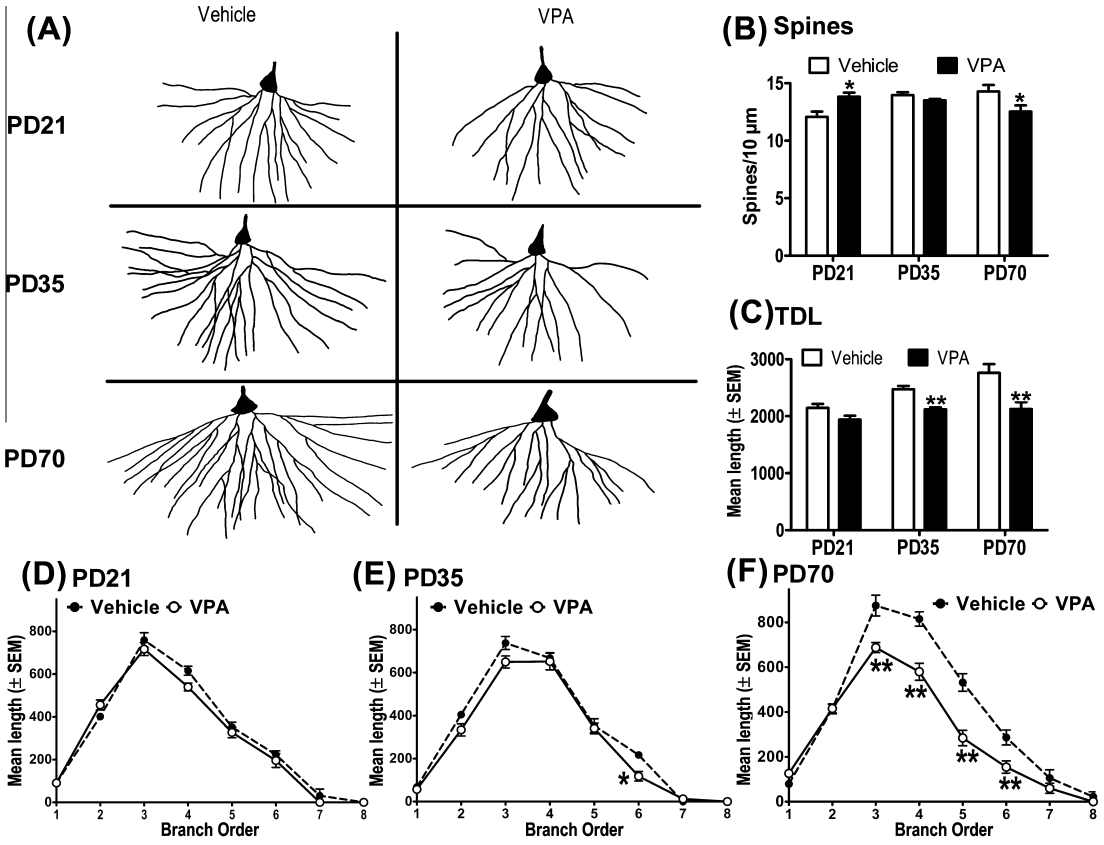

Fig. 8. The prenatal valproic acid (VPA) effect on the pyramidal neurons of the CA1 of the dorsal hippocampus immediately after weaning (PD21), in prepubertal (PD35) and in postpubertal (PD70) animals ($n = 8$ animals per group). (A) Representative schematic drawings of the dendritic basilar arbor of the dorsal hippocampus neurons. (B) Dendritic spiny neuron density. The density of the dendritic spines increased in VPA-treated animals compared to their corresponding vehicle rats at PD21, however at PD70, VPA-treated animals exhibited a reduced spinogenesis compared to their corresponding vehicle-treated animals. (C) Total dendritic length (TDL) analysis also revealed that VPA-treated rats showed an atrophy of the TDL at PD35 and PD70 compared to their corresponding vehicle animals. (D–F) Interestingly, length of branch-order analysis revealed that dendritic length of the CA1 of the dorsal hippocampus was shorter in the VPA-treated animals at the level of the third to fifth orders compared to their corresponding vehicle-treated rats. $^{*}P < 0.05$, $^{**}P < 0.01$.

Several reports have demonstrated that VPA injections at E12.5 yield autistic features in the rat (for review see Roullet et al., 2013), while earlier injections (E9.5) induce mostly teratogenic effects (Kim et al., 2011). In accordance with our results, Rinaldi et al. (2008), observed an increase in local connectivity specifically with neighboring neurons less than 50 µm away after VPA exposure (500 mg/kg) at E12.5 in the PFC. Pyramidal neurons of this cortex of young VPA-exposed animals showed marked abnormalities such as impaired intrinsic excitability and excessive NMDA synaptic currents (Rinaldi et al., 2007, 2008). Interestingly, using whole-cell patch recordings, Walcott et al. (2011) found that such abnormalities observed in pyramidal neurons of the PFC in VPA (500 mg/kg)-exposed rats peaked soon after birth, but were gradually corrected as animal matured, and normal excitability and NMDA currents were restored by early adolescence. In addition to that, in the present report we found that in some regions, the changes in the dendritic arborization and dendritic spines density were opposite at early age than after puberty. All together, these results suggest that homeostatic plasticity or compensatory mechanism(s) contribute to maintain stability and functionality of neural circuits in the face of challenges posed by developmental events in this animal model.

Prenatal VPA exposure increases locomotor activity and exploratory behavior assessed by hole-board test

Early age and postpubertal, but not peripubertal, animals prenatally exposed to VPA exhibit increased locomotor activity in a slightly stressful novel environment. This behavioral abnormalities are often related to increased mesolimbic-dopaminergic activity (Lipska et al., 1993; Flores et al., 1996a, 2005b; Wan et al., 1996; Brake et al., 1999; Chrapusta et al., 2003; Alquicer et al., 2004). The mechanism(s) by which VPA-exposure produces changes in hyper-responsiveness to stress at an early and postpubertal age without change at prepubertal (PD35) remains undetermined. However, several reports suggest that dopamine (DA) function change with age. An early report using autoradiography reveals that in the NAcc and CPu, the density of D1, D2, and D4 dopamine receptors increases to peak at postnatal day 28, and then declines significantly in both regions (PD35–60) to adult levels, whereas in the PFC

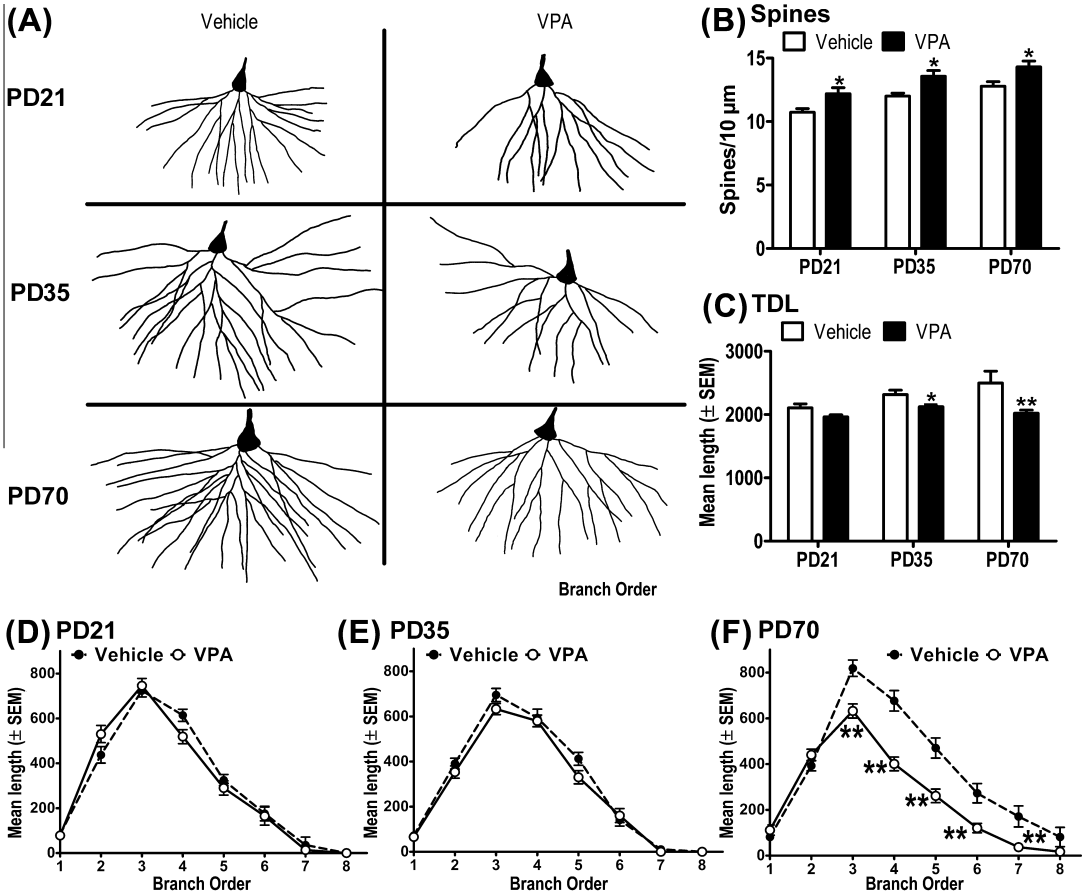

Fig. 9. The prenatal valproic acid (VPA) effect on the pyramidal neurons of the CA1 of the ventral hippocampus immediately after weaning (PD21), in prepubertal (PD35) and in postpubertal (PD70) animals (n = 8 animals per group). (A) Representative schematic drawings of the dendritic basilar arbor of the ventral hippocampus neurons. (B) Dendritic spine number analysis revealed that prenatal VPA exposure animals showed an enhanced spinogenesis compared to their corresponding vehicle rats at all ages. (C) In opposition, total dendritic length (TDL) analysis revealed that VPA-treated rats showed an atrophy of the TDL at PD35 and PD70 compared to their corresponding vehicle animals. (D–F) Interestingly, length of branch-order analysis revealed that dendritic length of the CA1 of the ventral hippocampus was shorter in the VPA-treated animals at the level of the third to seventh order compared to their corresponding vehicle-treated rats. $^{*}P < 0.05$, $^{**}P < 0.01$.

and hippocampus, stabilizes after reaching its maximum level at PD60 (Tarazi and Baldessarini, 2000). A recent report suggests a predominance of D2-like over D1-like function between 20 and 30 days of age (Chen et al., 2010). In addition, DA transporter (DAT) activity increased slightly from PN7 to PN14 and then increased more strongly to PN21, suggesting a higher DA release (Dreiem et al., 2009). Interestingly, an increase in vesicular DAT in periadolescent (PN 38–42) vs. young adult (PN88–92) rats is reported (for review see Volz et al., 2009). Furthermore, the DA reuptake inhibitor cocaine produces different behaviors and neurochemical effects in periadolescent vs. adult rats (Collins and Izenwasser, 2002). Additionally, several studies revealed that prenatal exposure to VPA increases DA levels in the PFC (Narita et al., 2002; Nakasato et al., 2008) with a decreased proenkephalin mRNA expression in the NAcc (Schneider et al., 2007). In light of the previous studies, our data are consistent with a hyperactive mesocortical DA system in rats prenatally exposed to VPA.

The hole-board test is a simple method for measuring the response of an animal to an unfamiliar environment (Boissier and Simon 1962). This test has been used to assess emotion, anxiety and/or response to stress in various animal models (File and Wardill, 1975; Rodriguez Echandia et al., 1987). Olfactory bulbectomy (OBX) has been used as a model of depression in the rat. Several reports suggest that the most consistent behavioral changes caused by OBX are hyperemotional responses (Kelly et al., 1997 and Morales-Medina et al., 2012), Interestingly, OBX produced hyperactivity in a novel environment with an increase in head-dipping behavior (Kamei et al., 2007). In addition, anti-anxiety drugs belonging to the family of benzodiazepines, such as chlordiazepoxide and diazepam, significantly increase exploration of a hole-board (for reviews see Crawley, 1985; Calabrese, 2008), whereas the opposite effect has been reported in animals with neonatal ventral hippocampus lesion, a neurodevelopmental model to mimic schizophrenia-like behaviors (Valdés-Cruz et al., 2012). In accordance with our results, significantly increased head-dip duration with less frequency implicated more exploratory behavior at PD70. Exploratory activity is a complex behavior involving several limbic structures (LaBerge, 2005; Simpson and

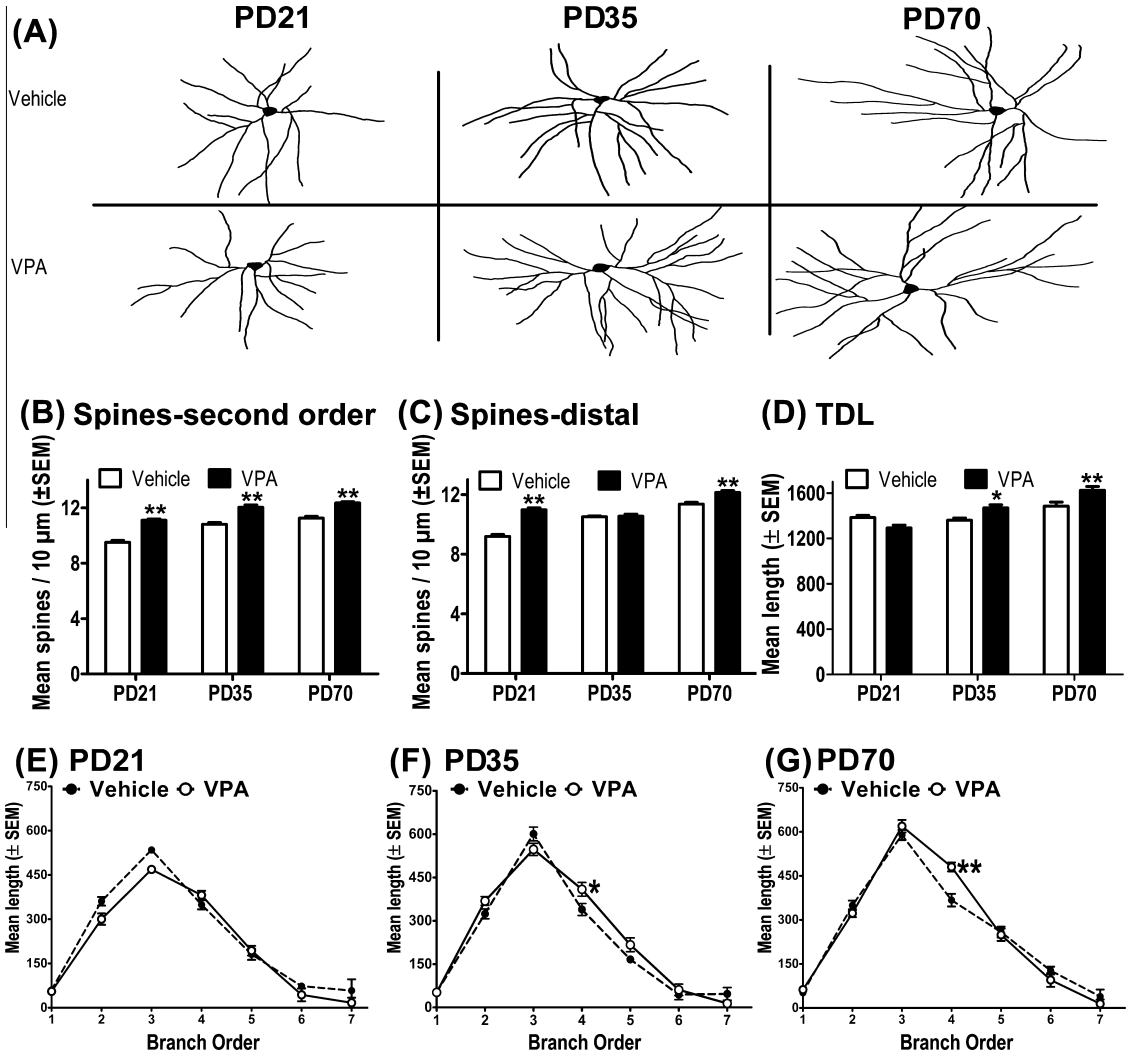

Fig. 10. The prenatal valproic acid (VPA) effect on the medium spiny neurons of the core part of the nucleus accumbens (NAcc-core) immediately after weaning (PD21), in prepubertal (PD35) and in postpubertal (PD70) animals ($n = 8$ animals per group). (A) Representative schematic drawings of the dendritic arbor of the medium spiny neurons of the NAcc-core. (B) Dendritic spine number analysis revealed that VPA-treated rats showed an enhanced spinogenesis at the level of the second order at all ages, whereas the distal dendritic spines also increase their number but only at PD21 and PD70 compared to their corresponding vehicle-treated animals. (C) Total dendritic length analysis revealed that VPA-treated rats showed a hypertrophy in the dendritic length compared to vehicle-treated animals at PD 35 and PD70 compared to their corresponding vehicle-treated rats. (D–F) Length of branch-order analysis revealed that VPA-treated nVHL rats showed a hypertrophy of the dendritic length at 3 branch order compared to their corresponding vehicle-treated group at PD 35 and PD70. $^{*}P < 0.05$, $^{**}P < 0.01$.

Kelly, 2011). For example, the intra-accumbens injection of a glutamatergic antagonist results in an increase in the exploratory activity measured by the hole-board test (Baiardi et al., 2007).

NAcc glutamatergic blockade has been reported to produce an increase in DA release in this nucleus (Carlsson et al., 1998). On the other hand, our recent report suggests that the lesion-induced loss of the inhibitory projections from the thalamic reticular nucleus (TRN) to the mediodorsal (MD) thalamus produces a reduction of the exploration time in the hole-board (Torres-García et al., 2012). In addition, the mesencephalic serotoninergic nuclei (dorsal and median raphe) have been implicated in the regulation of the head-dipping behavior assessed by hole-board test. Rats with median raphe nucleus lesion displayed high frequencies of head-dipping (Hoshino et al., 2004) whereas an increase in the time spent in head-dipping has been reported after dorsal raphe nucleus lesion in rats (Dray et al., 1978). Taken together, we propose that the dysfunction of the connections between hippocampus–PFC, PFC–NAcc, hippocampus–NAcc and BLA-Nacc due to prenatal VPA exposure may play a key role in the increase of impulsive-like behaviors observed in these rats compared to vehicle animals. We conclude that neonatal VPA administration may alter the connectivity among limbic structures, resulting in a dysfunction of the head-dipping behavior.

Cox–Golgi staining

The classical Golgi method for staining neurons in the brain was first developed by Camillio Golgi (Golgi, 1873, in Shepherd 1991). The original method is based on the

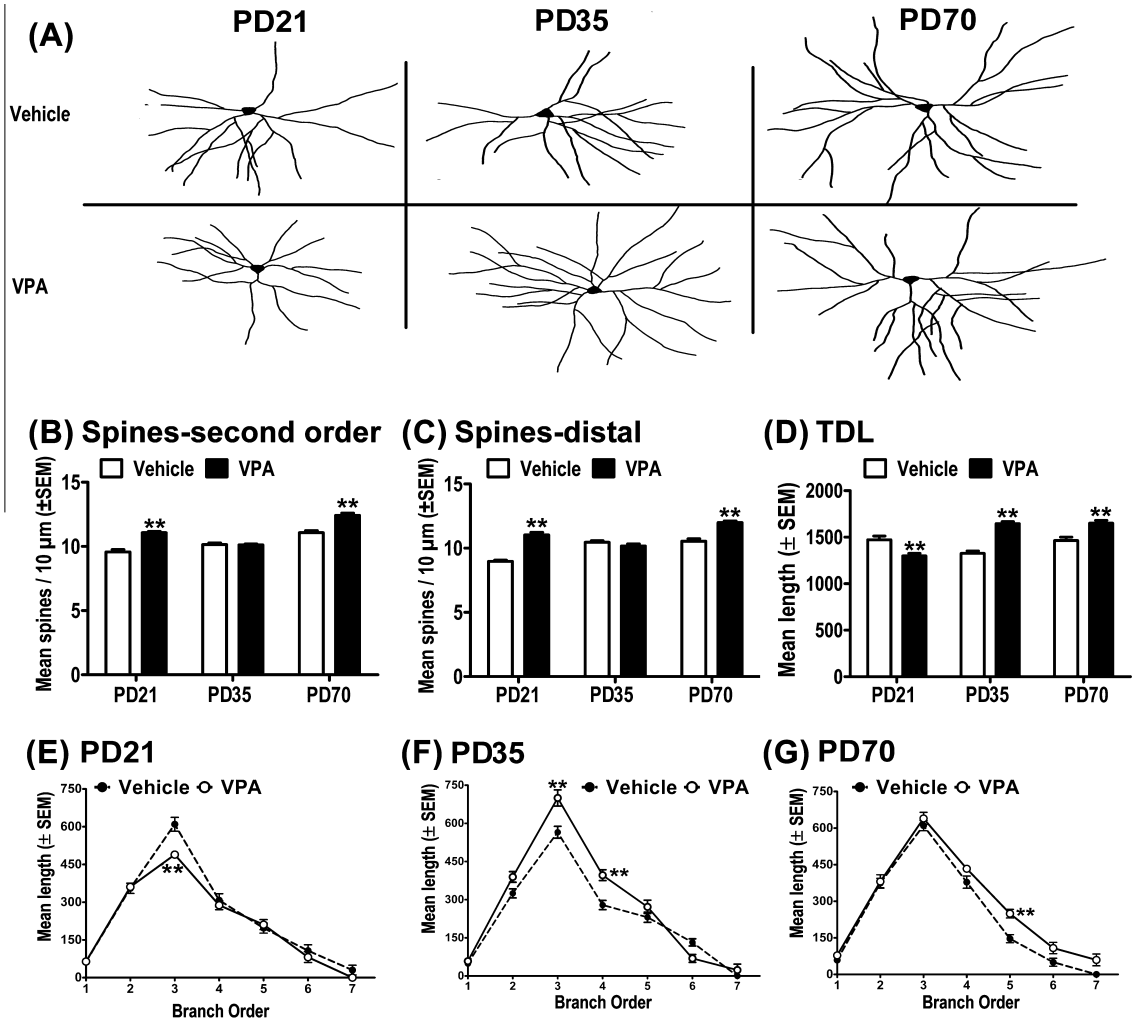

Fig. 11. The prenatal valproic acid (VPA) effect on the medium spiny neurons of the nucleus acumbens part shell (NAcc-shell) immediately after weaning (PD21), in prepubertal (PD35) and in postpubertal (PD70) animals (n = 8 animals per group). (A) Representative schematic drawings of the dendritic arbor of the medium spiny neurons of the NAcc-shell. (B) Dendritic spine number analysis of both regions, second order and distal to the soma, revealed that at PD21 and PD70, VPA rats showed an enhanced spinogenesis compared to their corresponding vehicle-treated animals. (C) Total dendritic length analysis revealed that VPA-treated rats showed a hypertrophy in the dendritic length at PD35 and PD70, but with initial reduction at PD21 compared to their corresponding vehicle-treated rats. (D–F) Length of branch-order analysis revealed that VPA-treated rats showed a hypertrophy of the dendritic length at 3 and 4 branches order at PD35 and at 6 branch order at PD70, with a reduced dendritic length at 3 branch order at PD21 compared to their corresponding vehicle-treated group. $^{*}P < 0.05$, $^{**}P < 0.01$.

formation of intracellular opaque deposits of silver chromate produced by the reaction between potassium dichromate and silver nitrate. Several modifications of the method have been made, such as in 1891, Cox used potassium chromate after the initial treatment with potassium dichromate and mercuric chloride, this variation to the Golgi method is known as Golgi–Cox method (Torres-Fernández, 2006). At the present, Golgi–Cox impregnation method has been used broadly to provide valuable information regarding the neural morphology (Gibb and Kolb, 1998; Flores et al., 2005a,b) and quantitative assessments such as dendritic spine number (Robinson and Kolb, 1999; Flores et al., 2005a; Melendez-Ferro et al., 2009; Kasture et al., 2009), dendritic length measurements and branching complexity (Flores et al., 2005a; Kolb et al., 1998). Interestingly, dendritic spines are known to be centers of information processing and are able to control their own protein synthesis and degradation (see as a review Halpain et al., 2005). These discrete dendritic protrusions form a rich structural scaffold for the majority of excitatory synapses in the brain (for review see Lee et al., 2012). In addition, Golgi–Cox method has been frequently used to stain neurons in both less myelinated, younger as well as in more myelinated, older rat brains. As compared to Golgi method, the advantage of Golgi–Cox method includes the increased probability of neuronal staining (Ranjan and Mallick, 2010).

Prenatal VPA exposure induced dendritic rearrangement in PFC, BLA, ventral and dorsal hippocampus and NAcc

The functional implications of these morphological changes remain unclear, especially with regard to

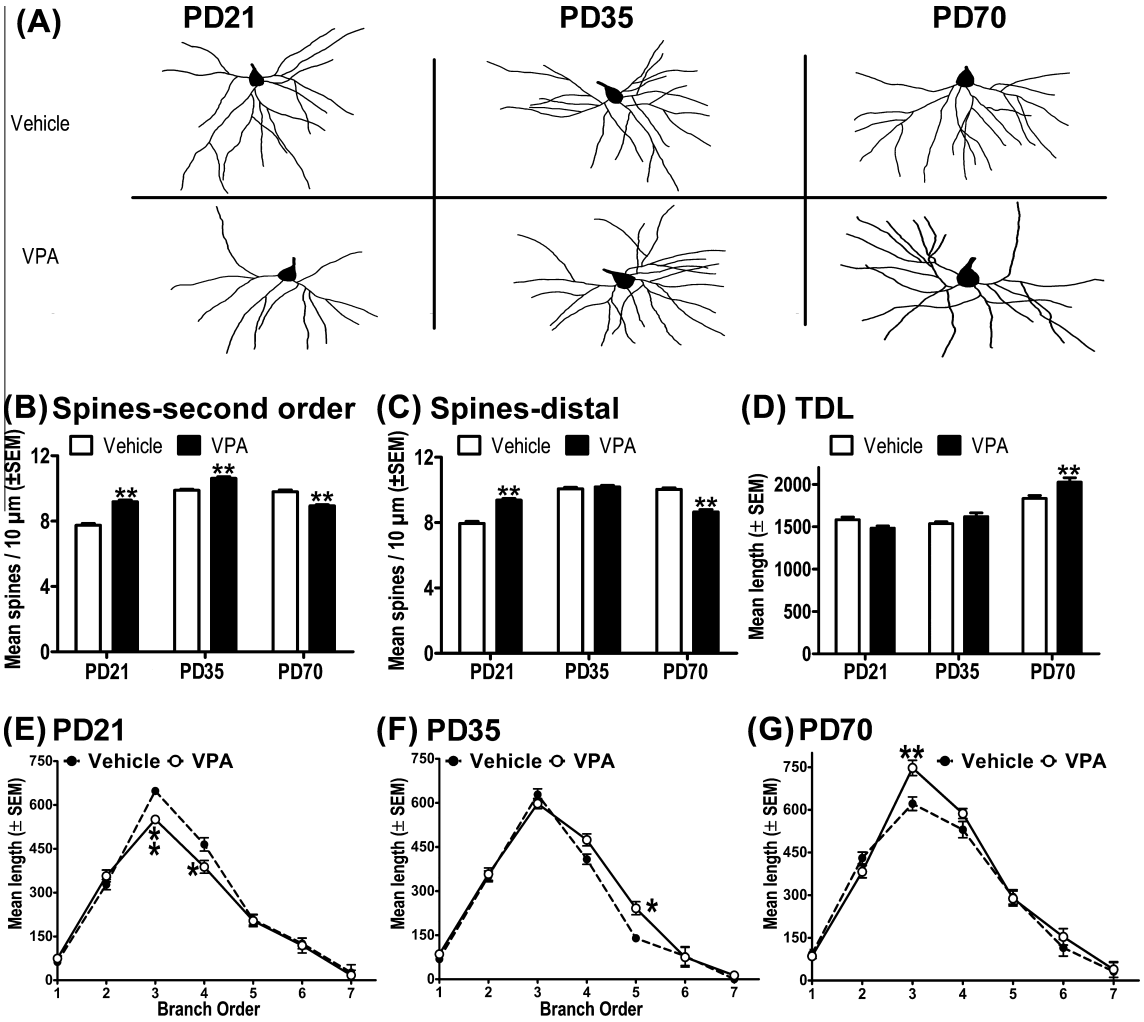

Fig. 12. The prenatal valproic acid (VPA) effect on the pyramidal neurons of the basolateral amygdala (BLA) immediately after weaning (PD21), in prepubertal (PD35) and in postpubertal (PD70) animals (n = 8 animals per group). (A) Representative schematic drawings of the dendritic basilar arbor of the BLA neurons. (B) Dendritic spine number analysis of both regions, second order and distal to the soma, revealed that at PD21, VPA rats showed an enhanced spinogenesis, but at PD70 showed a reduced spinogenesis, compared to their corresponding vehicle-treated animals. Interestingly, at PD35, only dendritic spines of the second order, also increased the number in the VPA animals. (C) Total dendritic length analysis revealed that VPA-treated rats showed a hypertrophy in the dendritic length at PD70 compared to their corresponding vehicle-treated rats. (D–F) Length of branch-order analysis revealed that VPA-treated rats showed a hypotrophy of the dendritic length at 3 and 4 branch order at PD21, however at PD35 and PD70, a hypertrophy of the fifth (PD35) and third (PD70) branches order were observed in the VPA rats compared to their corresponding vehicle-treated group. $^{*}P < 0.05$, $^{**}P < 0.01$.

whether dendritic retraction reflects detrimental or beneficial responses to the communication between limbic regions such as VH–PFC–NAcc or BLA–PFC–NAcc pathways. Common wisdom may dictate that dendritic loss could be interpreted as maladaptive plasticity. For example, studies in hippocampus and PFC neurons demonstrate that environmental deprivation-induced dendritic hypotrophy and spine loss are accompanied by cognitive impairments in tasks mediated by each respective structure (Silva-Gomez et al., 2003). In addition, dendritic retraction, reduced number of spines and cell loss of prefrontal cortical-pyramidal neurons has been recently reported in prenatal VPA rats at PD105 (Hara et al., 2012; Mychasiuk et al., 2012). In agreement with our results, recent report (Kolozsi et al., 2009) has shown that neonatal VPA exposure leads to a reduced expression of the synaptic adhesion molecule neuroligin 3, in adult mice. Neuroligins (NLGNs) are a family of postsynaptic cell-adhesion molecules that play a critical role in synaptic maturation (Ichtchenko et al., 1995, 1996; Shipman and Nicoll, 2012a,b). Interestingly, the trans-synaptic complex of NLGN and neurexin (NRXN) forms a physical connection between pre- and postsynaptic neurons that occurs early in the course of new synapse assembly. NLGN–NRXN interactions have been proposed to exhibit active, instructive roles in the formation of both inhibitory and excitatory synapses (for review see Craig and Kang, 2007; Südhof, 2008; Soler-Llavina et al., 2011). Furthermore, a recent report suggests that VPA-injection induces a transient histone hyper-acetylation immediately after administration,

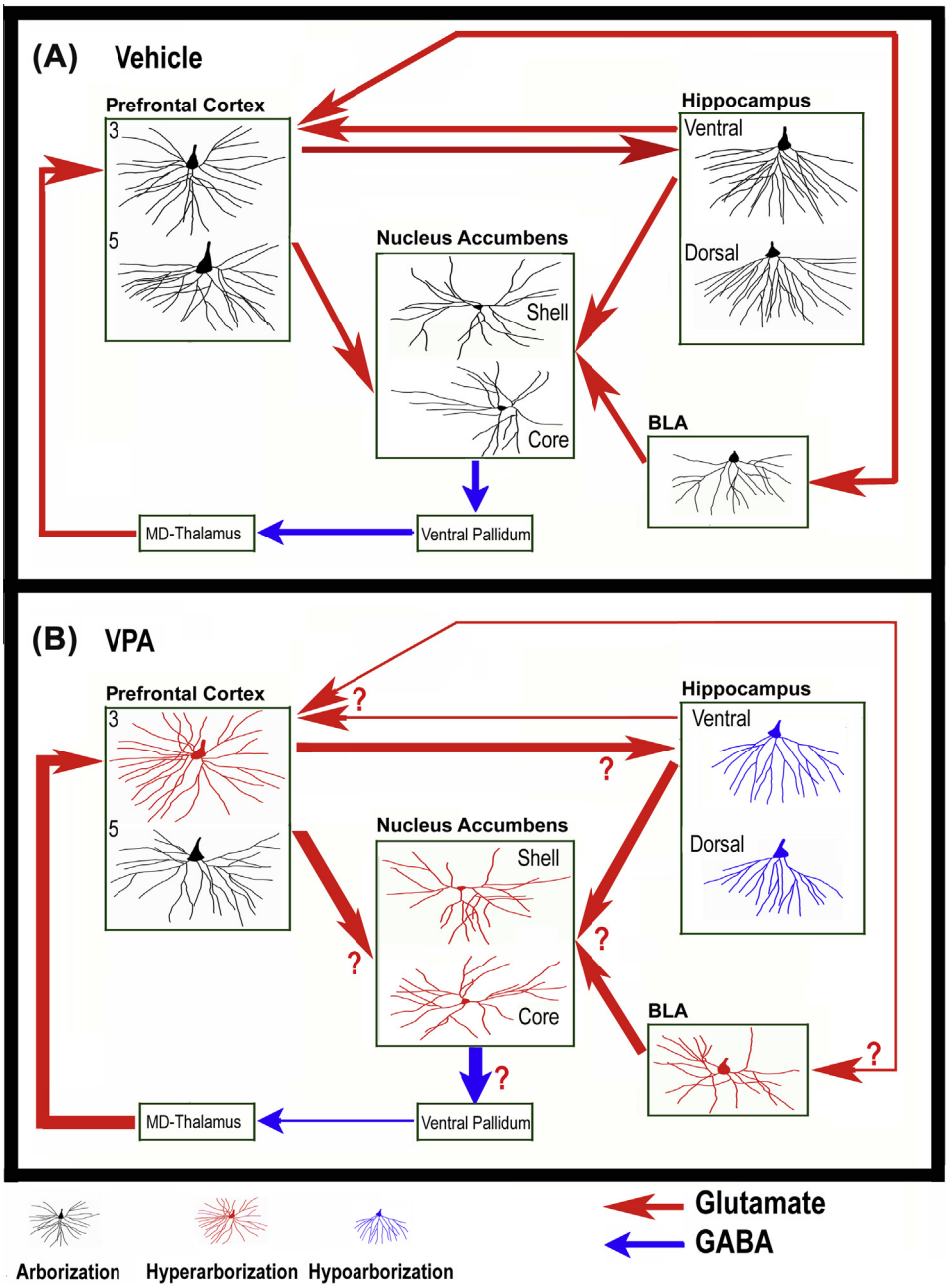

Fig. 13. Schematic illustration of main connections of the limbic system emphasizing the connection among prefrontal cortex (PFC), hippocampus, basolateral amygdala (BLA) and nucleus accumbens. Red arrows (A) In vehicle animals at PD70; (B) In prenatal VPA rats at PD70. The thickness of the arrow lines indicates the degree of excitatory connection (red) or inhibitory connection (blue).Other abbreviations: MD, mediodorsal, 3, layer 3 of the PFC; 5, layer 5 of the PFC. (For interpretation of the references to color in this figure legend, the reader is referred to the web version of this article.)

followed by increases in apoptotic cell death in the PFC (Kataoka et al., 2013). In addition, histone acetylation and deacetylation are responsible for maintaining chromatin stability (for review see Konsoula and Barile, 2012). These studies suggest that histone modifications in the brain may be an important factor in the generation of synaptic plasticity (Konsoula and Barile, 2012).

Interestingly, recent reports suggest sexual dimorphism in the behavioral and neural morphology in the VPA animal model (Hara et al., 2012; Mychasiuk et al., 2012; Kataoka et al., 2013). In fact, male, but not female, VPA animals show deficits in social interaction (Hara et al., 2012; Kataoka et al., 2013). Moreover, male VPA animals also show decreased number of Nissl-positive cell in the PFC and somatosensory cortex, whereas female offspring rats only exhibit a reduction in the Nissl-positive cell numbers in the PFC (Hara et al., 2012). In addition, a reduced dendritic branching in the

apical dendrites of the pyramidal neurons of the area Cingulate 3 was reported in the male but not female prenatally VPA-exposed rats (Mychasiuk et al., 2012). Therefore, the VPA animal model resembles human ASD, which similarly displays sex differences in behavior and neural morphology (Hall et al., 2012; Lai et al., 2012; Klusek et al., 2013).

The morphological changes observed in prenatally VPA-exposed animals at three critical ages (infantile, prepubertal and adult) are complex, and may be analyzed at least in two ways. First, as we mentioned before, dendritic spines are sites of synaptic contacts and likely represent measure of neuronal connectivity (for review see Kuwajima et al., 2012). In addition, distal dendritic spines may represent input from other anatomical areas. Therefore, in the prenatal VPA model, the pyramidal neurons of the PFC have a reduced excitatory input from the hippocampus and BLA at all studied ages. In contrast, medium spiny neurons of the NAcc received an enhanced excitatory input from the hippocampus, the PFC and the BLA resulting in reduced GABAergic drive from the ventral pallidum to MD thalamus (Fig. 13). Additionally the changes in dendritic arborization suggest that hyper-plasticity at the level of the neuronal dendritic arbor in the prenatal VPA model may result in local *over-connectivity* in BLA, PFC and NAcc circuitry, with local *under-connectivity* at the level of the VH and DH at PD70 (Fig. 13). Interestingly, several functional reports reveal that patients with ASD have deficits in long-distance connections (under-connectivity) (for review see Wass, 2011). In addition, with regard to structural connectivity, inter-hemispheric white matter structures have shown to be disrupted (for review see Palau-Baduell et al., 2012). Yet, the excess of local connections in ASD (over-connectivity), although considerably less documented, supports the hypothesis of the local over-connectivity in the patients with ASD (for review see Wass, 2011; Palau-Baduell et al., 2012).

Lastly, neuroimaging studies have revealed that neuro-psychiatric disorders are associated with various types of abnormalities in the hippocampus, PFC, and amygdala (for review see Charman et al.,2011; Kim et al., 2011; Calderoni et al., 2012). For example, in agreement with our data, a Golgi study from postmortem ASD patients suggests that pyramidal neurons of the CA1 hippocampus display less arborization compared to control samples (Raymond et al., 1996). In addition, histopathology abnormality has been reported in the amygdala from autism (Courchesne et al., 2001; Palmen et al., 2004), in which the neurons are smaller and more numerous and described as tightly packed. Our study allows to appreciate the range of developmental and region-specific alterations in a rat model of autism. A controversy still rages on the nature of synaptic alterations in ASD. While recent data converge to suggest that inhibitory synapses may be weakened in ASD, contrasting evidence and hypotheses indicate alternatively a hypo- or a hyper-synaptic connectivity of excitatory synapses: while older data, for instance like those from Horwitz et al. (1988) suggest hypo-connectivity of excitatory synapses, on the contrary, more recent data (Rinaldi et al., 2008; Silva et al., 2009; Testa-Silva et al., 2012) would suggest a glutamatergic system hyperconnectivity associated with ASD. Our morphological data suggest that a decrease in spine density in forebrain structures may be a substrate for distal hypo-connectivity, while the increase in dendritic length might support the enhancement of local hyperconnectivity, consistent with the ‘‘intense world’’ theory of ASD proposed by Markram and Markram (2010).

CONCLUSIONS

Our results suggest that the increase in the density of dendritic spines and reduced dendritic length (each in the areas where occurring) are consistent with the hypothesis that autism is associated with a local excitatory over-connectivity (excitatory neuron circuits near its source), and parallel to a reduction in long distance excitatory connections (from other anatomical areas).

CONFLICT OF INTEREST

All authors have no conflicts of interest.

FUNDING SOURCES

Funding for this study was provided by grants from VIEP-BUAP grant (No. FLAG-SAL12-Ind), PROMEP (CA-BUAP-120) and CONACYT grant (Nos. 129303 and 138663) to G. Flores. None of the funding institutions had any further role in the study design, the collection of data, analyses and interpretation of data, writing of the report or in the decision to submit the paper for publication and interpretation of data, writing of the report or the decision to submit the paper for publication.

CONTRIBUTORS

M.E.B., F.N.C.-F, T.A.L.-R., M.A. and G.F. design the study and wrote the protocol. M.E.B., F.N.C.-F. and T.A.L.-R. performed the experiments. M.E.B., M.A. and G.F. managed the literature searches and analysis, G.F. and M.A. undertook the statistical analysis and G.F. and M.A. wrote the first draft of the manuscript. All authors contributed and have approved the final manuscript.

Acknowledgements—The authors wish to thank Dr. Julio Cesar Morales-Medina for helpful comments and suggestions. Maria Elena Bringas was master student with a fellowship from CONACyT-Mexico. We also want to thank Dr. Carlos Escamilla for his help with the animal care. G.F. acknowledge the National Research System of Mexico for membership. The authors would like to thank Stephanie Newton for proofreading and editing the text.

REFERENCES

Alcantara-Gonzalez F, Juárez I, Solis O, Martínez-Téllez I, Camacho-Abrego I, Masliah E, Mena R, Flores G (2010) Enhanced dendritic spine number of neurons of the prefrontal cortex, hippocampus, and nucleus accumbens in old rats after chronic donepezil administration. Synapse 64:786–793.

Alquicer G, Silva-Gómez AB, Peralta F, Flores G (2004) Neonatal ventral hippocampus lesion alters the dopamine content in the limbic regions in postpubertal rats. Int J Dev Neurosci 22:103–111.

American Psychiatric Association (1994) Diagnostic and Statistical Manual of Mental Disorders. fourth ed. Washington: American Psychiatric Press.

Baiardi G, Ruiz AM, Beling A, Borgonovo J, Martínez G, Landa AI, Sosa MA, Gargiulo PA (2007) Glutamatergic ionotropic blockade within accumbens disrupts working memory and might alter the endocytic machinery in rat accumbens and prefrontal cortex. J Neural Transm 114:1519–1528.

Banerjee A, García-Oscos F, Hall S, Roychowdhury S, Galindo LC, Kilgard MP, Atzori M (2012) Impairment of cortical GABAergic synaptic transmission in an environmental rat model of autism. Int J Neuropsychopharmacol. http://dx.doi.org/10.1017/S1461145712001216.

Boissier JR, Simon P (1962) The exploration reaction in the mouse. Preliminary note. Therapie 17:1225–1232.

Brake WG, Sullivan RM, Flores G, Srivastava LK, Gratton A (1999) Neonatal ventral hippocampal lesions attenuate the nucleus accumbens dopamine response to stress: an electrochemical study in the adult rat. Brain Res 831:25–32.

Bringas ME, Morales-Medina JC, Flores-Vivaldo Y, Negrete-Diaz JV, Aguilar-Alonso P, León-Chávez BA, Lazcano-Ortiz Z, Monroy E, Rodríguez-Moreno A, Quirion R, Flores G (2012) Clozapine administration reverses behavioral, neuronal, and nitric oxide disturbances in the neonatal ventral hippocampus rat. Neuropharmacology 62:1848–1857.

Calabrese EJ (2008) An assessment of anxiolytic drug screening tests: hormetic dose responses predominate. Crit Rev Toxicol 38:489–542.

Calderoni S, Retico A, Biagi L, Tancredi R, Muratori F, Tosetti M (2012) Female children with autism spectrum disorder: an insight from mass-univariate and pattern classification analyses. Neuroimage 59:1013–1022.

Carlsson A, Hansson LO, Waters N, Carlsson ML (1998) A glutamatergic deficiency model of schizophren. Br J Psychiatry 173(Suppl. 37):2–6.

Casanova M, Trippe J (2009) Radial cytoarchitecture and patterns of cortical connectivity in autism. Philos Trans R Soc Lond B Biol Sci 364:1433–1436.

Charman T, Jones CR, Pickles A, Simonoff E, Baird G, Happé F (2011) Defining the cognitive phenotype of autism. Brain Res 1380:10–21.

Chen L, Liu J, Zhan QJ, Feng JJ, Gui ZH, Al U, Wang Y, Fan LL, Hou C, Wang T (2011) Alterations of emotion, cognition and firing activity of the basolateral nucleus of the amygdala after partial bilateral lesions of the nigrostriatal pathway in rats. Brain Res Bull 85:329–338.

Chen YI, Choi JK, Xu H, Ren J, Andersen SL, Jenkins BG (2010) Pharmacologic neuroimaging of the ontogeny of dopamine receptor function. Dev Neurosci 32:125–138.

Chrapusta SJ, Egan MF, Wyatt RJ, Weinberger DR, Lipska BK (2003) Neonatal ventral hippocampal damage modifies serum corticosterone and dopamine release responses to acute footshock in adult Sprague–Dawley rats. Synapse 47: 270–277.

Collins SL, Izenwasser S (2002) Cocaine differentially alters behavior and neurochemistry in periadolescent versus adult rats. Brain Res Dev Brain Res 138:27–34.

Courchesne E, Karns CM, Davis HR, Ziccardi R, Carper RA, Tigue ZD, Chisum HJ, Moses P, Pierce K, Lord C, Lincoln AJ, Pizzo S, Schreibman L, Haas RH, Akshoomoff NA, Courchesne RY (2001) Unusual brain growth patterns in early life in patients with autistic disorder: an MRI study. Neurology 57:245–254.

Craig AM, Kang Y (2007) Neurexin–neuroligin signaling in synapse development. Curr Opin Neurobiol 17:43–52.

Crawley JN (1985) Exploratory behavior models of anxiety in mice. Neurosci Biobehav Rev 9:37–44.

Denys D, Zohar J, Westenberg HG (2004) The role of dopamine in obsessive–compulsive disorder: preclinical and clinical evidence. J Clin Psychiatry 65(Suppl. 14):11–17.

Dreiem A, Shan M, Okoniewski RJ, Sanchez-Morrissey S, Seegal RF (2009) Methylmercury inhibits dopaminergic function in rat pup synaptosomes in an age-dependent manner. Neurotoxicol Teratol 31:312–317.

Dray A, Davies J, Oakley NR, Tongroach P, Vellucci S (1978) The dorsal and medial raphe projections to the substantia nigra in the rat: electrophysiological, biochemical and behavioural observations. Brain Res 151:431–442.

Dufour-Rainfray D, Vourc'h P, Le Guisquet AM, Garreau L, Ternant D, Bodard S, Jaumain E, Gulhan Z, Belzung C, Andres CR, Chalon S, Guilloteau D (2010) Behavior and serotonergic disorders in rats exposed prenatally to valproate: a model for autism. Neurosci Lett 470:55–59.

File SE, Wardill AG (1975) The reliability of the hole-board apparatus. Psychopharmacologia 44:47–51.

Flores G, Barbeau D, Quirion R, Srivastava LK (1996a) Decreased binding of dopamine D3 receptors in limbic subregions after neonatal bilateral lesion of rat hippocampus. J Neurosci 16: 2020–2026.

Flores G, Wood GK, Liang JJ, Quirion R, Srivastava LK (1996b) Enhanced amphetamine sensitivity and increased expression of dopamine D2 receptors in postpubertal rats after neonatal excitotoxic lesions of the medial prefrontal cortex. J Neurosci 16:7366–7375.

Flores G, Alquicer G, Silva-Gómez AB, Zaldivar G, Stewart J, Quirion R, Srivastava LK (2005a) Alterations in dendritic morphology of prefrontal cortical and nucleus accumbens neurons in post-pubertal rats after neonatal excitotoxic lesions of the ventral hippocampus. Neuroscience 133:463–470.

Flores G, Silva-Gómez AB, Barbeau D, Srivastava LK, Zamudio S, De La Cruz López F (2005b) Comparative behavioral changes in postpubertal rats after neonatal excitotoxic lesions of the ventral hippocampus and the prefrontal cortex. Synapse 56:147–153.

Flores-Tochihuitl J, Vargas G, Morales-Medina JC, Rivera G, De La Cruz F, Zamudio S, Flores G (2008) Enhanced apomorphine sensitivity and increased binding of dopamine D2 receptors in nucleus accumbens in prepubertal rats after neonatal blockade of the dopamine D3 receptors by (+)-S14297. Synapse 62:40–49.

Gibb R, Kolb B (1998) A method for vibratome sectioning of Golgi–Cox stained whole rat brain. J Neurosci Methods 79:1–4.

Halpain S, Spencer K, Graber S (2005) Dynamics and pathology of dendritic spines. Prog Brain Res 147:29–37.

Hall J, Philip RC, Marwick K, Whalley HC, Romaniuk L, McIntosh AM, Santos I, Sprengelmeyer R, Johnstone EC, Stanfield AC, Young AW, Lawrie SM (2012) Social cognition, the male brain and the autism spectrum. PLoS One 7:e49033. http://dx.doi.org/10.1371/journal.pone.0049033.

Hara Y, Maeda Y, Kataoka S, Ago Y, Takuma K, Matsuda T (2012) Effect of prenatal valproic acid exposure on cortical morphology in female mice. J Pharmacol Sci 118:543–546.

Horwitz B, Rumsey JM, Grady CL, Rapoport SI (1988) The cerebral metabolic landscape in autism. Intercorrelations of regional glucose utilization. Arch Neurol 45:749–755.

Hoshino K, Uga DA, de Paula HM (2004) The compulsive-like aspect of the head dipping emission in rats with chronic electrolytic lesion in the area of the median raphe nucleus. Braz J Med Biol Res 37:245–250.

Ichtchenko K, Hata Y, Nguyen T, Ullrich B, Missler M, Moomaw C, Südhof TC (1995) Neuroligin 1: a splice site-specific ligand for beta-neurexins. Cell 81:435–443.

Ichtchenko K, Nguyen T, Südhof TC (1996) Structures, alternative splicing, and neurexin binding of multiple neuroligins. J Biol Chem 271:2676–2682.

Ingram JL, Peckham SM, Tisdale B, Rodier PM (2000) Prenatal exposure of rats to valproic acid reproduces the cerebellar anomalies associated with autism. Neurotoxicol Teratol 22: 319–324.

Jay TM, Witter MP (1991) Distribution of hippocampal CA1 and subicular efferents in the prefrontal cortex of the rat studied by means of anterograde transport of *Phaseolus vulgaris*-leucoagglutinin. J Comp Neurol 313:574–586.

Juárez I, Gratton A, Flores G (2008) Ontogeny of altered dendritic morphology in the rat prefrontal cortex, hippocampus, and nucleus accumbens following Cesarean delivery and birth anoxia. J Comp Neurol 507:1734–1747.

Kamei J, Hirose N, Oka T, Miyata S, Saitoh A, Yamada M (2007) Effects of methylphenidate on the hyperemotional behavior in olfactory bulbectomized mice by using the hole-board test. J Pharmacol Sci 103:175–1780.

Kasture S, Vinci S, Ibba F, Puddu A, Marongiu M, Murali B, Pisanu A, Lecca D, Zernig G, Acquas E (2009) *Withania somnifera* prevents morphine withdrawal-induced decrease in spine density in nucleus accumbens shell of rats: a confocal laser scanning microscopy study. Neurotox Res 16:343–355.

Kataoka S, Takuma K, Hara Y, Maeda Y, Ago Y, Matsuda T (2013) Autism-like behaviours with transient histone hyperacetylation in mice treated prenatally with valproic acid. Int J Neuropsychopharmacol 16:91–103.

Kelly JP, Wrynn AS, Leonard BE (1997) The olfactory bulbectomized rat as a model of depression: an update. Pharmacol Ther 74:299–316.

Kim MJ, Loucks RA, Palmer AL, Brown AC, Solomon KM, Marchante AN, Whalen PJ (2011) The structural and functional connectivity of the amygdala: from normal emotion to pathological anxiety. Behav Brain Res 223:403–410.

Klusek J, Losh M, Martin GE (2013) Sex differences and within-family associations in the broad autism phenotype. Autism. http://dx.doi.org/10.1177/1362361312464529.

Kolb B, Stewart J, Sutherland RJ (1997) Recovery of function is associated with increased spine density in cortical pyramidal cells after frontal lesions and/or noradrenaline depletion in neonatal rats. Behav Brain Res 89:61–70.

Kolb B, Forgie M, Gibb R, Gorny G, Rowntree S (1998) Age, experience and the changing brain. Neurosci Biobehav Rev 22:143–159.

Kolozsi E, Mackenzie RN, Roullet FI, de Catanzaro D, Foster JA (2009) Prenatal exposure to valproic acid leads to reduced expression of synaptic adhesion molecule neuroligin 3 in mice. Neuroscience 163:1201–1210.

Konsoula Z, Barile FA (2012) Epigenetic histone acetylation and deacetylation mechanisms in experimental models of neurodegenerative disorders. J Pharmacol Toxicol Methods 66:215–220.

Kuwajima M, Spacek J, Harris KM (2012) Beyond counts and shapes: studying pathology of dendritic spines in the context of the surrounding neuropil through serial section electron microscopy. Neuroscience. http://dx.doi.org/10.1016/j.bbr.2011.03.031.

LaBerge D (2005) Sustained attention and apical dendrite activity in recurrent circuits. Brain Res Brain Res Rev 50:86–99.

Lai MC, Lombardo MV, Ruigrok AN, Chakrabarti B, Wheelwright SJ, Auyeung B, Allison C, MRC AIMS Consortium, Baron-Cohen S (2012) Cognition in males and females with autism: similarities and differences. PLoS One 7:e47198. http://dx.doi.org/10.1371/journal.pone.0047198.

Lauvin MA, Martineau J, Destrieux C, Andersson F, Bonnet-Brilhault F, Gomot M, El-Hage W, Cottier JP (2012) Functional morphological imaging of autism spectrum disorders: current position and theories proposed. Diagn Interv Imaging 3:139–1347.

Lee KF, Soares C, Béïque JC (2012) Examining form and function of dendritic spines. Neural Plast 2012:704103. http://dx.doi.org/10.1155/2012/704103.

Lipska BK, Jaskiw GE, Weinberger DR (1993) Postpubertal emergence of hyperresponsiveness to stress and to amphetamine after neonatal excitotoxic hippocampal damage: a potential animal model of schizophrenia. Neuropsychopharmacology 9:67–75.

Markram K, Markram H (2010) The intense world theory – a unifying theory of the neurobiology of autism. Front Hum Neurosci 4:224.

Martínez-Téllez RI, Hernández-Torres E, Gamboa C, Flores G (2009) Prenatal stress alters spine density and dendritic length of nucleus accumbens and hippocampus neurons in rat offspring. Synapse 63:794–804.

McCracken JT, McGough J, Shah B, Cronin P, Hong D, Aman MG, Arnold LE, Lindsay R, Nash P, Hollway J, McDougle CJ, Posey D, Swiezy N, Kohn A, Scahill L, Martin A, Koenig K, Volkmar F, Carroll D, Lancor A, Tierney E, Ghuman J, Gonzalez NM, Grados M, Vitiello B, Ritz L, Davies M, Robinson J, McMahon D, Research Units on Pediatric Psychopharmacology Autism Network () (2002) Risperidone in children with autism and serious behavioral problems. N Engl J Med 347:314–321.

Melendez-Ferro M, Perez-Costas E, Roberts RC (2009) A new use for long-term frozen brain tissue: golgi impregnation. J Neurosci Methods 176:72–77.

Miyazaki K, Narita N, Narita M (2005) Maternal administration of thalidomide or valproic acid causes abnormal serotonergic neurons in the offspring: implication for pathogenesis of autism. Int J Dev Neurosci 23:287–297.

Monroy E, Hernández-Torres E, Flores G (2010) Maternal separation disrupts dendritic morphology of neurons in prefrontal cortex, hippocampus, and nucleus accumbens in male rat offspring. J Chem Neuroanat 40:93–101.

Morales-Medina JC, Dumont Y, Benoit CE, Bastianetto S, Flores G, Fournier A, Quirion R (2012) Role of neuropeptide Y Y1 and Y2 receptors on behavioral despair in a rat model of depression with co-morbid anxiety. Neuropharmacology 62:200–208.

Morales-Medina JC, Sanchez F, Flores G, Dumont Y, Quirion R (2009) Morphological reorganization after repeated corticosterone administration in the hippocampus, nucleus accumbens and amygdala in the rat. J Chem Neuroanat 38:266–272.

Mychasiuk R, Richards S, Nakahashi A, Kolb B, Gibb R (2012) Effects of rat prenatal exposure to valproic acid on behaviour and neuro-anatomy. Dev Neurosci 34:268–276.

Nakasato A, Nakatani Y, Seki Y, Tsujino N, Umino M, Arita H (2008) Swim stress exaggerates the hyperactive mesocortical dopamine system in a rodent model of autism. Brain Res 1193:128–135.

Narita N, Kato M, Tazoe M, Miyazaki K, Narita M, Okado N (2002) Increased monoamine concentration in the brain and blood of fetal thalidomide- and valproic acid-exposed rat: putative animal models for autism. Pediatric Res:576–579.

Palmen SJ, van Engeland H, Hof PR, Schmitz C (2004) Neuropathological findings in autism. Brain 127:2572–2583.

Palau-Baduell M, Salvadó-Salvadó B, Clofent-Torrentó M, Valls-Santasusana A (2012) Autism and neural connectivity. Rev Neurol 29(54 Suppl. 1):S31–S39.

Paxinos G, Watson C (1986) The Rat Brain in Stereotaxic Coordinates. New York: Academic Press.

Ranjan A, Mallick BN (2010) A modified method for consistent and reliable Golgi–Cox staining in significantly reduced time. Front Neurol 1:157. http://dx.doi.org/10.3389/fneur.2010.00157.

Raymond GV, Bauman ML, Kemper TL (1996) Hippocampus in autism: a Golgi analysis. Acta Neuropathol 91:117–119.

Rinaldi T, Kulangara K, Antoniello K, Markram H (2007) Elevated NMDA receptor levels and enhanced postsynaptic long-term potentiation induced by prenatal exposure to valproic acid. Proc Natl Acad Sci U S A 104:13501–13506.

Rinaldi T, Perrodin C, Markram H (2008) Hyper-connectivity and hyper-plasticity in the medial prefrontal cortex in the valproic acid animal model of autism. Front Neural Circuits 2:4. http://dx.doi.org/10.3389/neuro.04.004.2008.

Rippon G, Brock J, Brown C, Boucher J (2007) Disordered connectivity in the autistic brain: challenges for the ‘‘new psychophysiology’’. Int J Psychophysiol 63:164–172.

Robinson TE, Kolb B (1999) Alterations in the morphology of dendrites and dendritic spines in the nucleus accumbens and prefrontal cortex following repeated treatment with amphetamine or cocaine. Eur J Neurosci 11:1598–15604.

Rodier PM, Ingram JL, Tisdale B, Croog VJ (1997) Linking etiologies in humans and animal models: studies of autism. Reprod Toxicol 11:417–422.

Rodriguez Echandia EL, Broitman ST, Fóscolo MR (1987) Effect of the chronic ingestion of chlorimipramine and desipramine on the hole board response to acute stresses in male rats. Pharmacol Biochem Behav 26:207–210.

Roullet FI, Lai JK, Foster JA (2013) In utero exposure to valproic acid and autism – a current review of clinical and animal studies. Neurotoxicol Teratol. http://dx.doi.org/10.1016/j.ntt.2013.01.004.

Schneider T, Przewłocki R (2005) Behavioral alterations in rats prenatally exposed to valproic acid: animal model of autism. Neuropsychopharmacology 30:80–89.

Schneider T, Turczak J, Przewłocki R (2006) Environmental enrichment reverses behavioral alterations in rats prenatally exposed to valproic acid: issues for a therapeutic approach in autism. Neuropsychopharmacology 31:36–46.

Schneider T, Ziołkowska B, Gieryk A, Tyminska A, Przewłocki R (2007) Prenatal exposure to valproic acid disturbs the enkephalinergic system functioning, basal hedonic tone, and emotional responses in an animal model of autism. Psychopharmacology 193:547–555.

Shalom DB (2009) The medial prefrontal cortex and integration in autism. Neuroscientist 15:589–598.

Shepherd GM (1991) Foundations of the Neuron Doctrine. New York: Oxford University Press.

Shipman SL, Nicoll RA (2012a) Dimerization of postsynaptic neuroligin drives synaptic assembly via transsynaptic clustering of neurexin. Proc Natl Acad Sci U S A 109:19432–19437.

Shipman SL, Nicoll RA (2012b) A subtype-specific function for the extracellular domain of neuroligin 1 in hippocampal LTP. Neuron 76:309–316.

Sholl DA (1953) Dendritic organization in the neurons of the visual and motor cortices of the cat. J Anat 87:387–406.

Silva GT, Le Bé JV, Riachi I, Rinaldi T, Markram K, Markram H (2009) Enhanced long-term microcircuit plasticity in the valproic acid animal model of autism. Front Synaptic Neurosci 1:1.

Silva-Gomez AB, Rojas D, Juárez I, Flores G (2003) Decreased dendritic spine density on prefrontal cortical and hippocampal pyramidal neurons in postweaning social isolation rats. Brain Res 983:128–136.

Simpson J, Kelly JP (2011) The impact of environmental enrichment in laboratory rats – behavioural and neurochemical aspects. Behav Brain Res 222:246–264.

Snow WM, Hartle K, Ivanco TL (2008) Altered morphology of motor cortex neurons in the VPA rat model of autism. Dev Psychobiol 50(7):633–639.

Soler-Llavina GJ, Fuccillo MV, Ko J, Südhof TC, Malenka RC (2011) The neurexin ligands, neuroligins and leucine-rich repeat transmembrane proteins, perform convergent and divergent synaptic functions in vivo. Proc Natl Acad Sci U S A 10840: 16502–16509.

Südhof TC (2008) Neuroligins and neurexins link synaptic function to cognitive disease. Nature 455:903–911.

Sui L, Chen M (2012) Prenatal exposure to valproic acid enhances synaptic plasticity in the medial prefrontal cortex and fear memories. Brain Res Bull 87:556–563.

Tarazi FI, Baldessarini RJ (2000) Comparative postnatal development of dopamine D(1), D(2) and D(4) receptors in rat forebrain. Int J Dev Neurosci 18:29–37.

Testa-Silva G, Loebel A, Giugliano M, de Kock CP, Mansvelder HD, Meredith RM (2012) Hyperconnectivity and slow synapses during early development of medial prefrontal cortex in a mouse model for mental retardation and autism. Cereb Cortex 22:1333–1342.

Thompson L, Thompson M, Reid A (2010) Functional neuroanatomy and the rationale for using EEG biofeedback for clients with Asperger's syndrome. Appl Psychophysiol Biofeedback 35: 39–61.

Torres-Fernández O (2006) The Golgi silver impregnation method: commemorating the centennial of the Nobel Prize in medicine (1906) shared by Camillo Golgi and Santiago Ramón y Cajal. Biomedica 26:498–508.

Torres-García ME, Solis O, Patricio A, Rodríguez-Moreno A, Camacho-Abrego I, Limón ID, Flores G (2012) Dendritic morphology changes in neurons from the prefrontal cortex, hippocampus and nucleus accumbens in rats after lesion of the thalamic reticular nucleus. Neuroscience 223:429–438.

Valdés-Cruz A, Negrete-Díaz JV, Magdaleno-Madrigal VM, Martínez-Vargas D, Fernández-Mas R, Salvador Almazán-Alvarado S, Torres-García ME, Flores G (2012) Electroencephalographic activity in neonatal ventral hippocampus lesion in adult rats. Synapse 66:738–746.

Volz TJ, Farnsworth SJ, Rowley SD, Hanson GR, Fleckenstein AE (2009) Age-dependent differences in dopamine transporter and vesicular monoamine transporter-2 function and their implications for methamphetamine neurotoxicity. Synapse 63:147–151.

Wagner GC, Reuhl KR, Cheh M, McRae P, Halladay AK (2006) A new neurobehavioral model of autism in mice: pre- and postnatal exposure to sodium valproate. J Autism Dev Disord 36:779–793.

Walcott EC, Higgins EA, Desai NS (2011) Synaptic and intrinsic balancín during postnatal development in rat pups exposed to valproic acid in utero. J Neurosci 31:13097–13109.

Wan RQ, Giovanni A, Kafka SH, Corbett R (1996) Neonatal hippocampal lesions induced hyperresponsiveness to amphetamine: behavioral and in vivo microdialysis studies. Behav Brain Res 78:211–223.

Wass S (2011) Distortions and disconnections: disrupted brain connectivity in autism. Brain Cogn 75:18–28.

(Accepted 15 March 2013)
(Available online 25 March 2013)